ESC-TR-2001-071

Project Report
EO-1-10

Earth Observing-1 Advanced Land Imager Flight Performance Assessment: Absolute Radiometry and Stability During the First Year

J.A. Mendenhall
D.E. Lencioni

31 May 2002

Lincoln Laboratory
MASSACHUSETTS INSTITUTE OF TECHNOLOGY
LEXINGTON, MASSACHUSETTS

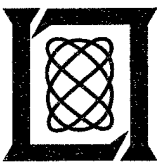

Prepared for the National Aeronautics and Space Administration under Air Force Contract F19628-00-C-0002.

This report is based on studies performed at Lincoln Laboratory, a center for research operated by Massachusetts Institute of Technology. This work was sponsored by NASA/Goddard Space Flight Center under Air Force Contract F19628-00-C-0002. Opinions, interpretations, conclusions, and recommendations are those of the authors and are not necessarily endorsed by the United States Air Force.

The ESC Public Affairs Office has reviewed this report, and it is releasable to the National Technical Information Service, where it will be available to the general public, including foreign nationals.

This technical report has been reviewed and is approved for publication.

FOR THE COMMANDER

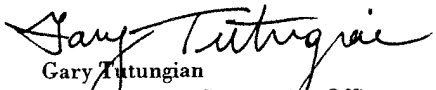

Gary Tutungian
Administrative Contracting Officer
Plans and Programs Directorate
Contracted Support Management

Massachusetts Institute of Technology
Lincoln Laboratory

Earth Observing-1 Advanced Land Imager Flight Performance Assessment: Absolute Radiometry and Stability During the First Year

J.A. Mendenhall
D.E. Lencioni
Group 99

Project Report EO-1-10

31 May 2002

Lexington Massachusetts

ABSTRACT

The absolute radiometry of the Advanced Land Imager during the first year on orbit (November 21, 2000–November 21, 2001) is presented. Results derived from solar, lunar, ground truth, and internal reference lamp measurements are presented. An 18% drop in the radiometric response of the Band 1p data since preflight calibration at Lincoln Laboratory is observed using all techniques. This decrease cannot be accounted for by preflight calibration errors, stray light, or contamination of the focal plane. A slight drooping of the VNIR response toward the blue and a 5–12% increase in the Band 5 response is also apparent in all the data. Radiometric response correction factors have been calculated and preflight calibration coefficients have been updated in order to provide ±5% agreement between the measured solar, lunar, and ground truth data and the expected values.

The radiometric stability of the ALI during the first year of operation is also presented for each spectral band. Internal reference lamp data indicate the focal plane has been stable to within 1% for bands 1p, 1, 2, 5p, 5, 7, pan and 3% for Bands 3, 4, 4p since launch. Solar, lunar, and ground truth measurements indicate the optical train and solar diffuser of the instrument has been stable to within 1% since initial measurements on orbit in late December 2000.

TABLE OF CONTENTS

1	INTRODUCTION		1
2	ABSOLUTE RADIOMETRY		3
	2.1	Solar Calibration	3
	2.2	Ground Truth	6
	2.3	Lunar Calibration	7
	2.4	Internal Reference Lamp Illumination	9
3	RADIOMETRIC STABILITY		11
	3.1	Solar Calibration	14
	3.2	Ground Truth	16
	3.3	Lunar Calibration	17
	3.4	Internal Reference Lamp Illumination	17
	3.5	Comparison of Results	19
4	DISCUSSION		31
	4.1	Sources of Radiometric Differences	31
	4.2	Stability	34
	4.3	Calibration Methods	35
	REFERENCES		37

LIST OF ILLUSTRATIONS

Figure		Page
1.	Illustration of the solar calibration mode and laboratory test data from a solar simulator.	3
2.	Measured detector responses for the ten ALI bands during a solar calibration.	4
3.	BRDF of diffuser located in front of the ALI secondary mirror.	5
4.	Results of solar calibration of the ALI from February 9, 2001.	5
5.	Overlay of ground truth results obtained by the University of Arizona and solar calibration data.	7
6.	Image of the Moon taken by the ALI on February 7, 2001.	8
7.	Results from solar, ground truth, and lunar absolute radiometric calibrations.	9
8.	EO-1 ALI internal reference source.	10
9.	Photograph of internal reference source.	10
10.	Radiometric calibration measurement periods.	12
11.	Effects of contamination on Band 3 data.	13
12.	Solar calibration correction factors.	15
13.	Instrument response stability for Band 3 based on solar calibration data.	15
14.	Change in instrument response for Band 3 derived from solar calibration data.	16
15.	Instrument response stability for Band 3 based on ground truth measurements.	16
16.	Instrument response stability for Band 3 based on lunar calibration measurements.	17
17.	Instrument response stability based on internal reference lamp data.	18
18.	Change in instrument response for Band 3 derived from internal reference lamp data.	18
19.	Trending of ALI radiometric calibration data for Band 1p.	19
20.	Trending of ALI radiometric calibration data for Band 1.	20
21.	Trending of ALI radiometric calibration data for Band 2.	20
22.	Trending of ALI radiometric calibration data for Band 3.	21
23.	Trending of ALI radiometric calibration data for Band 4.	21
24.	Trending of ALI radiometric calibration data for Band 4p.	22
25.	Trending of ALI radiometric calibration data for Band 5p.	22
26.	Trending of ALI radiometric calibration data for Band 5.	23
27.	Trending of ALI radiometric calibration data for Band 7.	23
28.	Trending of ALI radiometric calibration data for Pan Band.	24
29.	Radiometric stability of detectors for Band 1p as determined by internal lamp and solar calibration data collected during the first year on orbit.	25
30.	Radiometric stability of detectors for Band 1 as determined by internal lamp and solar calibration data collected during the first year on orbit.	25
31.	Radiometric stability of detectors for Band 2 as determined by internal lamp and solar calibration data collected during the first year on orbit.	26
32.	Radiometric stability of detectors for Band 3 as determined by internal lamp and solar calibration data collected during the first year on orbit.	26

LIST OF ILLUSTRATIONS (Continued)

Figure		Page
33.	Radiometric stability of detectors for Band 4 as determined by internal lamp and solar calibration data collected during the first year on orbit.	27
34.	Radiometric stability of detectors for Band 4p as determined by internal lamp and solar calibration data collected during the first year on orbit.	27
35.	Radiometric stability of detectors for Band 5p as determined by internal lamp and solar calibration data collected during the first year on orbit.	28
36.	Radiometric stability of detectors for Band 5 as determined by internal lamp and solar calibration data collected during the first year on orbit.	28
37.	Radiometric stability of detectors for Band 7 as determined by internal lamp and solar calibration data collected during the first year on orbit.	29
38.	Radiometric stability of detectors for the panchromatic band as determined by internal lamp and solar calibration data collected during the first year on orbit.	29
39.	Band 3 radiometric error model and flight data.	33
40.	Results of ALI absolute radiometric calibration after the corrections to pre-flight calibration coefficients are applied.	34

LIST OF TABLES

Table		Page
1.	Dates of EO-1 ALI on-orbit radiometric calibrations.	11
2.	Radiometric corrections (%) used to remove contamination effects.	13
3.	Radiometric stability trending results for first year on orbit.	24
4.	Radiometric correction factors used to update preflight calibration coefficients.	33

1. INTRODUCTION

The Advanced Land Imager (ALI) is a technology demonstration instrument for future wide field-of-view, pushbroom, land-imaging systems[1, 2]. One key area of this demonstration is stable, accurate absolute radiometry. This document provides a review of the absolute radiometry of the ALI during the first 12 months on-orbit (November 21, 2000–November 21, 2001). Included in this analysis are a description of the various on-orbit radiometric calibration techniques employed and a comparison of absolute radiometric levels derived from each method. The stability of the ALI is also presented for each band.

2. ABSOLUTE RADIOMETRY

The radiometric accuracy of the ALI has been tracked using several methods including solar calibration, ground truth measurements, lunar observations, and internal reference lamp illumination.

2.1 SOLAR CALIBRATION

Solar calibration of the ALI is conducted approximately every fourteen days. The solar calibration procedure, which is illustrated in Figure 1, involves pointing the ALI at the Sun with the aperture cover closed[3]. A motor-driven aperture selector in the aperture cover assembly moves an opaque slide over a row of small to increasingly larger slit openings and then reverses the slide motion to block all sunlight. Just prior to solar calibration, a space grade Spectralon® diffuser plate is swung over the secondary mirror by a motor-driven mechanism. The diffuser reflectively scatters the sunlight that would otherwise impinge on the secondary mirror. The scattered sunlight exposes the FPA to irradiance levels equivalent to Earth-reflected sunlight for albedos ranging from 0 to 100%.

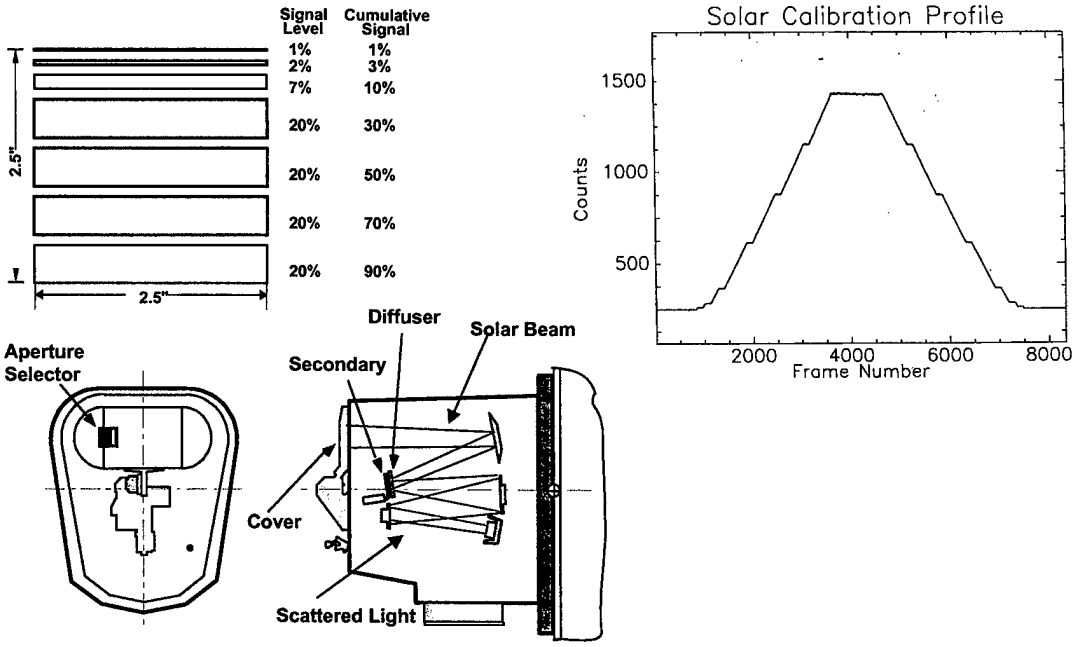

Figure 1. Illustration of the solar calibration mode and laboratory test data from a solar simulator.

The detector response during a solar calibration sequence consists of an approximately linear increase as the aperture opens, with a series of constant responses during those times when the slide passes over a reference bar. These bars provide a set of seven calibrated response points. When the aperture cover reverses direction and closes, the pattern of response reverses and proceeds back down to zero. Typical examples of detector responses for each of the ten ALI spectral bands are shown in Figure 2.

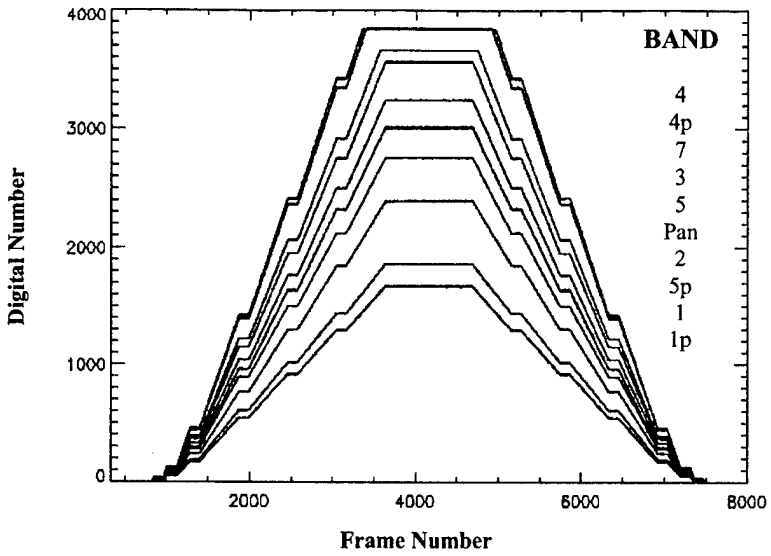

Figure 2. Measured detector responses for the ten ALI bands during a solar calibration.

The flux level at the maximum or seventh level corresponds approximately to a 100% albedo at a 30° solar zenith angle.

During solar calibration, the optical throughput of the ALI differs from a normal data collection because the Spectralon BRDF replaces the reflectance of the secondary mirror. Measurements of the BRDF were made on a spare flight quality Spectralon disk over a spectral range of 400 to 900 nm and for the appropriate angles of incidence and reflection at NASA's Goddard Space Flight Center. Values outside this spectral range were estimated by assuming that they scale as the total hemispherical reflectance, which was measured by Labsphere®. The resulting BRDF is shown in Figure 3.

A detailed CODE V® optical analysis provided the ratios of the irradiance at the FPA to the solar irradiance at the sub aperture for each position of the aperture selector. For a given sub aperture, the FPA irradiance was shown to vary by 2% over the full 15-degree field of view and by less than 1% over the region populated by detectors. The irradiance at the FPA is thus a known function of the aperture slot opening and solar irradiance. This FPA irradiance corresponds to a known effective radiance at ALI entrance. The detector channel output (DN) corresponding to this effective radiance provides the solar calibration.

The solar irradiance model used in the analysis is the MODTRAN 4.0–CHKUR model, which is currently being used for all Landsat 7 solar calibration derived gains.

The results from a solar calibration measurement, performed on February 9, 2001, are provided in Figure 4. The measured radiances using pre-launch calibration coefficients[4] for each band have been normalized to the expected values from the Code V analysis. These data are plotted at the mean wavelength of each band.

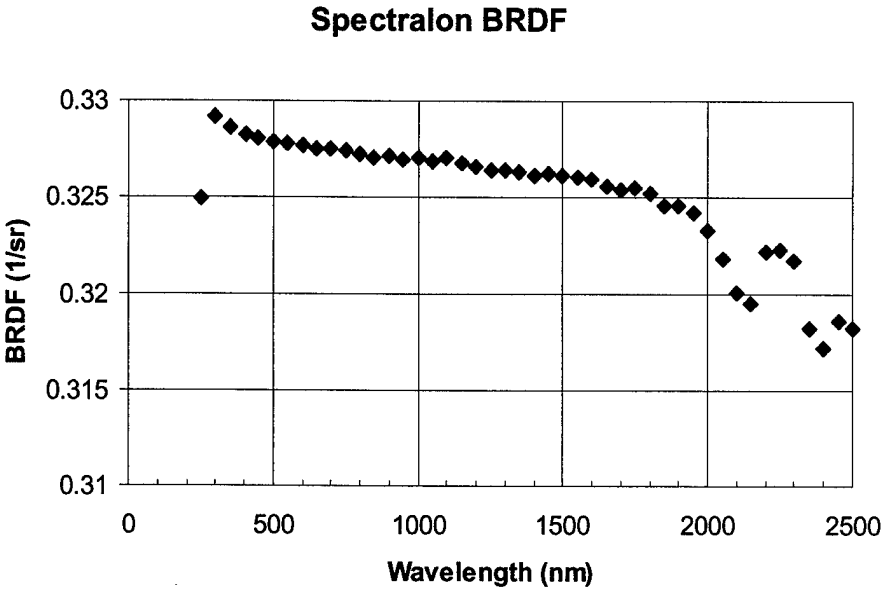

Figure 3. BRDF of diffuser located in front of the ALI secondary mirror used in the solar calibration model.

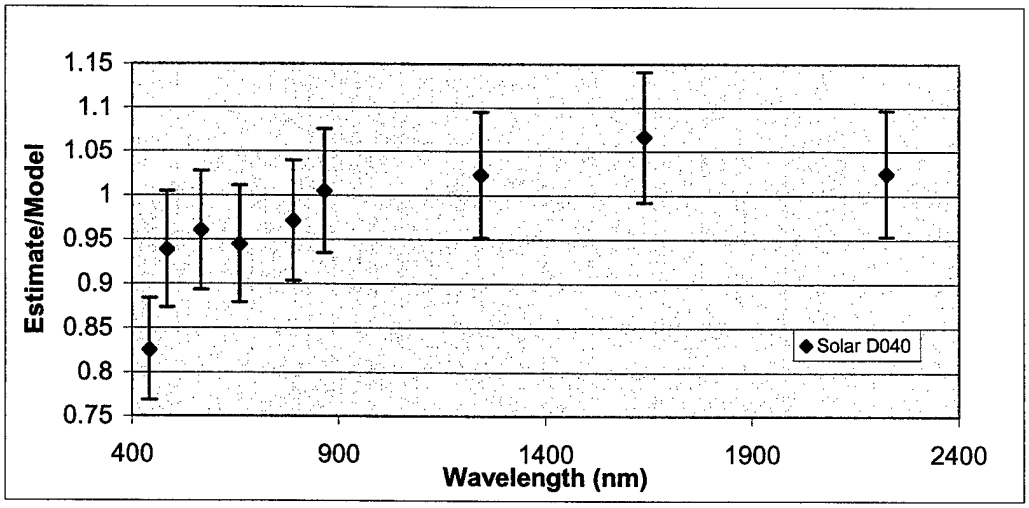

Figure 4. Results of solar calibration of the ALI from February 9, 2001. The ratio of observed to expected radiances for level 6 are plotted as a function of wavelength.

With the exception of band 1p, the solar and pre-launch calibrations agree to within the estimated uncertainties. The pre-launch calibration error, combined with the additional on-orbit effects of contamination and stray light, is estimated to be less than 5% for all bands. The solar calibration uncertainty is estimated to be 5% in the VNIR bands and 7% in the SWIR bands. The larger uncertainty in the SWIR bands is due to both the uncertainty in the solar irradiance models and the BRDF of the Spectralon. The low response in band 1p is a significant discrepancy between the two calibration techniques. A potential cause for this discrepancy is the degradation of the Spectralon diffuser, which is known to be highly susceptible to contamination. This hypothesis

was ruled out by comparing the solar calibration results to lunar calibration measurements and ground truth observations.

The solar calibration data exhibit two other interesting trends, which are of lesser significance. There is a general increase in the ratios with increasing wavelength as can be seen in Figure 4. A second effect, not shown here, is a decrease in the ratio with decreasing aperture area. The effect has been attributed to a systematic error (within machining tolerances) in the aperture areas.

2.2 GROUND TRUTH

The second method of assessing the radiometric accuracy of ALI data hinges on reflectance-based ground truth measurements[5]. The principle of this technique is to image a stable, high-altitude, flat, diffuse ground target using the ALI while simultaneously measuring the reflective properties of the target region and local atmospheric conditions. The ground measurements can then be used to predict the top of the atmosphere radiance observed by the ALI.

Throughout the first year of the EO-1 mission, ground truth campaigns were conducted by several groups, including the University of Arizona, the University of Colorado, the Australian CSIRO, and the NASA Jet Propulsion Laboratory. Ground truth sites include Barreal Blanco and Arizario Argentina, Lake Frome Australia, and complementary sites in the western United States (Railroad Valley, Ivanpah Playa, Walnut Gulch, and White Sands).

The first step of the reflectance-based approach is to measure the reflectivity of the site to be imaged by the ALI. This consists of obtaining several spectroradiometric measurements of a sample portion of the site by walking a backpack-mounted sensor in a grid-like manner and averaging the results. Immediately prior to and after these measurements, spectroradiometric measurements of a lambertian reference panel are obtained. The reflectance of the site is then obtained by ratioing the average site radiance to the average panel radiance and interpolating the result to the 1 nm level.

The second step of the reflectance-based approach is to measure the local atmospheric conditions at the time of the EO-1 overflight. Data obtained from a multispectral solar radiometer are used as input to atmospheric modeling tools to retrieve spectral atmospheric optical depths in 1 nm intervals from 400–2500 nm, aerosol size distribution, and column water vapor levels.

Once the surface reflectance and atmospheric conditions have been measured, a top of the atmosphere radiance is predicted at the time of the EO-1 overflight. First, the solar irradiance impinging on the Earth's atmosphere is determined from a solar irradiance model and Sun-Earth distance. Next, the effects of atmospheric scatter and absorption are accounted for using radiative transfer modeling. The downwelling irradiance is then reflected off the site surface using the reflectivity measurements obtained previously. The atmospheric scatter and absorption effects on the upwelling radiance are accounted for by additional radiative transfer modeling, resulting in a predicted hyperspectral at-sensor radiance. Finally, the integrated product of the predicted hyperspectral radiance and ALI spectral response functions provides expected in-band radiances for the site for each spectral band. The predicted in-band radiances are then compared to the observed in-band radiances, based on pre-flight calibration, in order to evaluate the absolute radiometry of the instrument.

Figure 5 overlays the results of ground truth measurements of Barreal Blanco, Argentina and Ivanpah Playa, California obtained by the Remote Sensing Group of the University of Arizona[6] with the solar calibration measurement presented earlier. The errors associated with the ground truth measurements have been estimated to be ±3%.

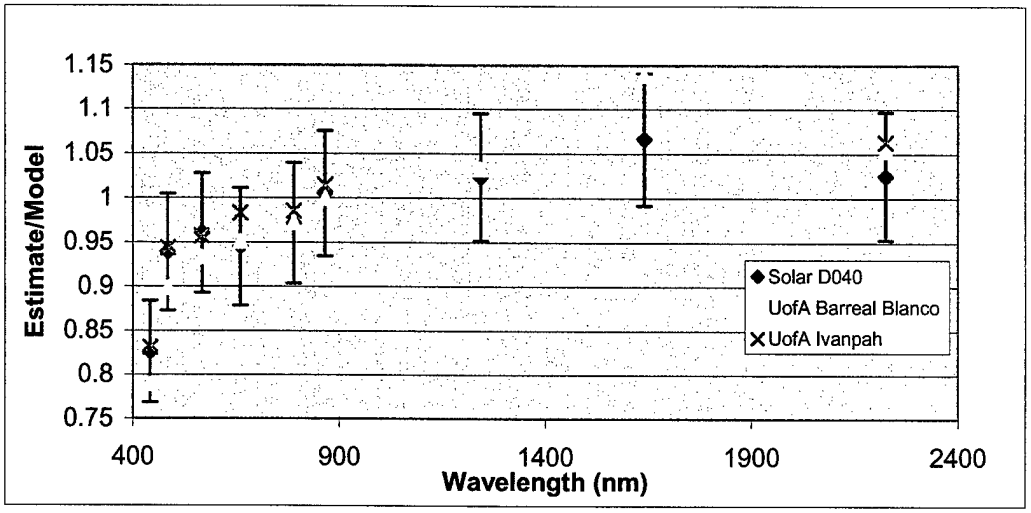

Figure 5. Overlay of ground truth results obtained by the University of Arizona and solar calibration data.

Examination of Figure 5 reveals good agreement between the ground truth and solar calibration measurements. The repeatability of the Band 1p offset and overall trend in the VNIR add confidence to the solar calibration model and indicate a change in the ALI radiometric response since pre-flight calibration for these bands. However, a 7% difference between the solar and ground truth data exists for Band 5 (1650 nm) and is not well understood at this time.

2.3 LUNAR CALIBRATION

A third method used to evaluate the absolute radiometry of the ALI on orbit is lunar calibration. This method involves observing the Moon with the instrument and comparing the measured lunar spectral irradiance with a predicted lunar irradiance for the time of the observation.

Lunar observations using the ALI have been conducted near a 7° phase angle each month since January 2001. For each observation, the spacecraft is maneuvered to scan the Moon in the in-track direction at 1/8 the nominal scan rate in order to oversample the disk. Because the Moon has ~½° diameter, the entire lunar disk may be imaged on an individual sensor chip assembly or SCA. As a result, four images of the Moon are obtained during each lunar calibration sequence—one per SCA.

To calculate the observed lunar irradiance, dark current levels are subtracted and the image is radiometrically calibrated using the pre-flight calibration coefficients. A region of interest, narrowly circumscribing the Moon, is then defined by locating the region of each column where the intensity falls to below 1% of the average lunar irradiance (Figure 6).

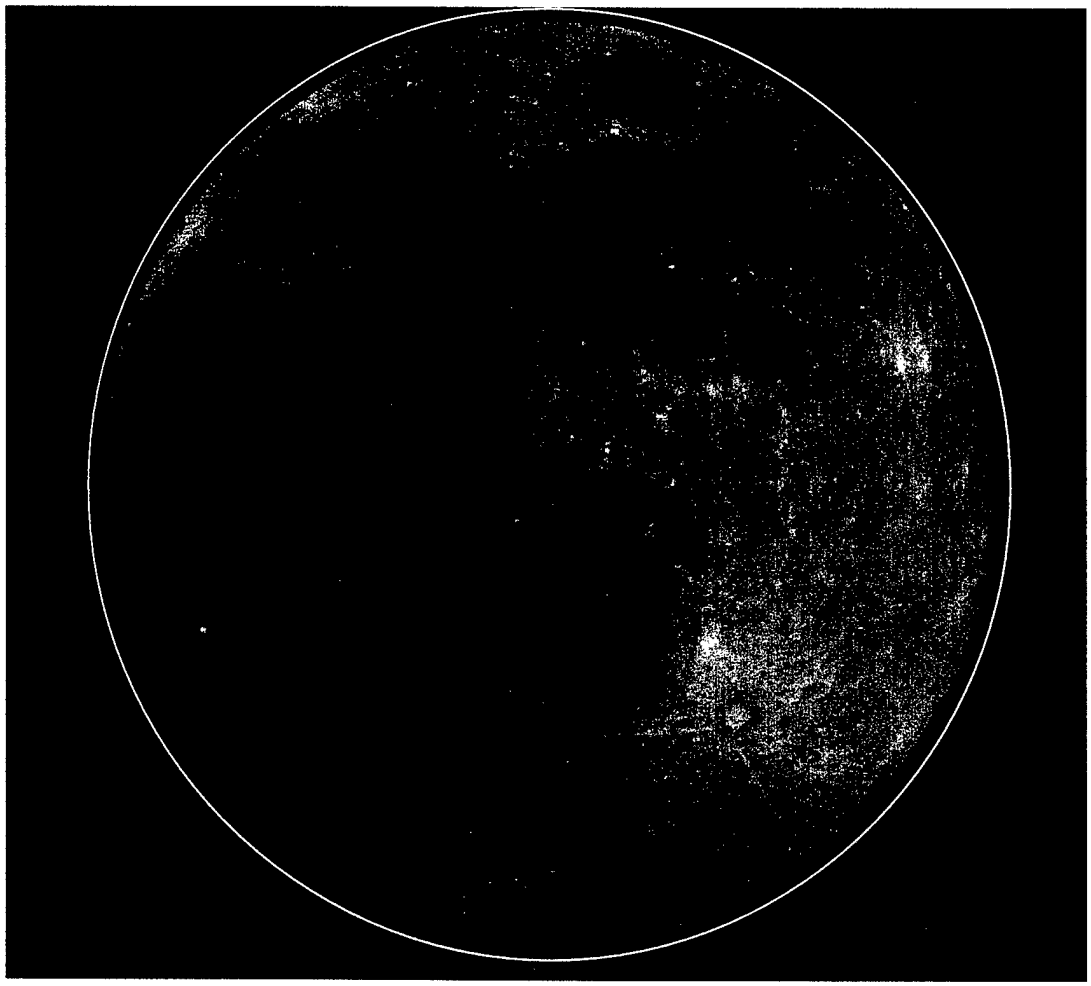

Figure 6. Image of the Moon taken by the ALI on February 7, 2001. The circle surrounding the Moon defines the regions used in the lunar irradiance calculations.

Summing the response within the circumscribed region, the spectral irradiance of the Moon for each band may be calculated as

$$E_M(\lambda, day) = \frac{d\Theta\Delta}{fF}\Sigma L_P(\lambda)$$

Here, E_M (λ,day) is the lunar spectral irradiance for a given mission day number, $d\Theta$ is the ALI pitch rate during the scan (radians/second), Δ is the detector pitch, f is the ALI focal length, F is the frame rate (Hz), and L_P (λ) is the measured lunar spectral radiance for detector P ($mW/cm^2/sr/\mu m$).

Once the measured lunar irradiance has been determined for a given observation, the expected lunar irradiance is calculated by the USGS using data obtained from the Robotic Lunar Observatory (ROLO) in Flagstaff, Arizona[7]. Since 1996 ROLO has been measuring the lunar irradiance between 350 and 2500 nm as a function of phase angle as often as weather and seeing permit. Contemporaneous observations of nearby bright stars provide absolute calibration of the Observatory, as well as a measurement of atmospheric extinction. The USGS has been able to use this database to predict lunar irradiance for most phase angles. As a result, lunar observations are emerging as an exciting new opportunity for radiometric calibration of space based VNIR/SWIR instruments.

The results of a lunar irradiance comparison for measurements obtained on February 7, 2001 required a normalization of 5% to the ROLO data for all bands in order to bring the results into agreement with ALI measurements. The source of this offset is unclear at this time but the leading candidate is an uncertainty in the absolute radiometric traceability of the ROLO measurements (the absolute radiometry of the ROLO observations are currently being reviewed). However, once the 5% offset is applied, the lunar irradiance comparison result was overlaid with solar and ground truth comparisons (Figure 7). The lunar data agree well with the other techniques, supporting the hypothesis that the radiometric response of the instrument has changed significantly for Band 1p and has drooped slightly in the VNIR since pre-flight measurements were taken.

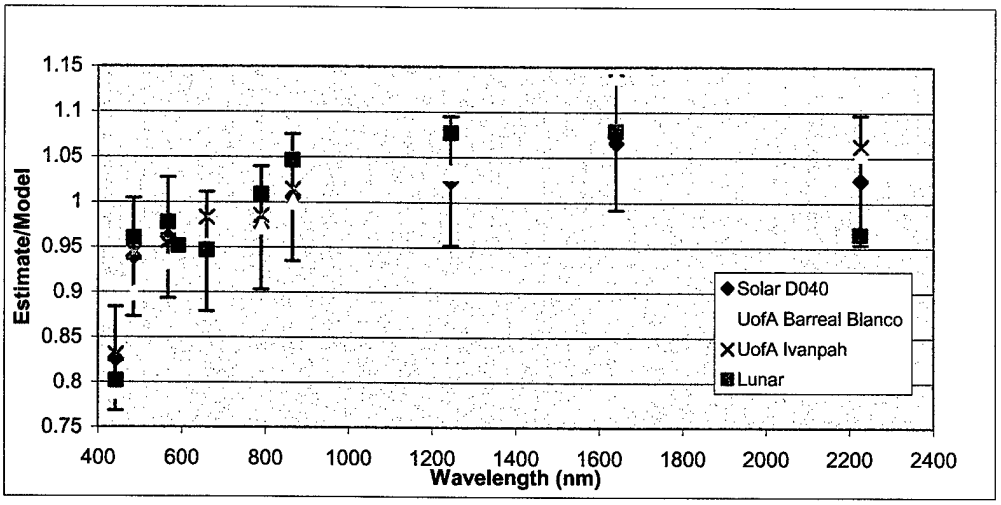

Figure 7. Results from solar, ground truth, and lunar absolute radiometric calibrations.

2.4 INTERNAL REFERENCE LAMP ILLUMINATION

Another source of on-orbit radiometric calibration for the ALI is an internal reference source mounted on the inside of the telescope. This source consists of three Welch Allyn 997418-7 (modified) gas-filled lamps mounted on a small (2.03 cm) diameter integrating sphere (Figures 8 and 9). Light emerging from the exit slit of the sphere passes through a BK 7 lens and infrared filter, is reflected off the ALI flat mirror (M4), and floods the focal plane.

The internal reference lamps are activated during two data collection events per day, when the ALI aperture cover is closed. After an eight-second stabilization period the lamps are sequentially powered down in a staircase fashion, with two-second exposures between each step. In this manner, the focal plane will receive a daily three point radiometric reference.

Initially, the internal reference source was to serve as a radiometric transfer standard between pre-flight and on-orbit calibrations of the ALI. However, a noticeable increase in lamp output in the VNIR was observed immediately after launch. This has been attributed to a loss of convective cooling of the filament in the zero-G environment. This increase in lamp output has resulted in invalidating attempts at using the reference lamps as a calibration transfer standard between preflight and flight calibration of the ALI detector arrays. However, the lamp output has been very repeatable since launch and has proven to be invaluable at monitoring the stability of the focal plane during the first year of on-orbit operations.

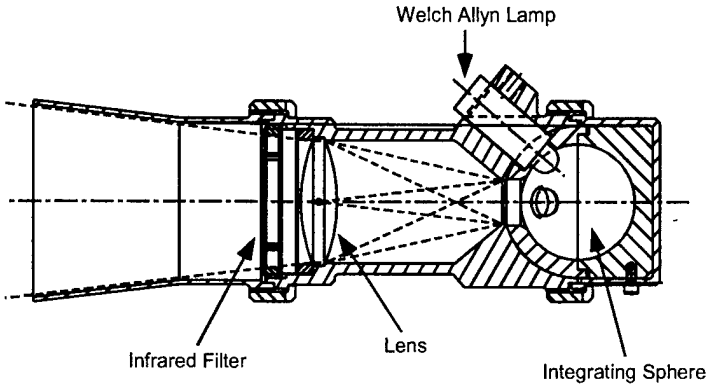

Figure 8. EO-1 ALI internal reference source.

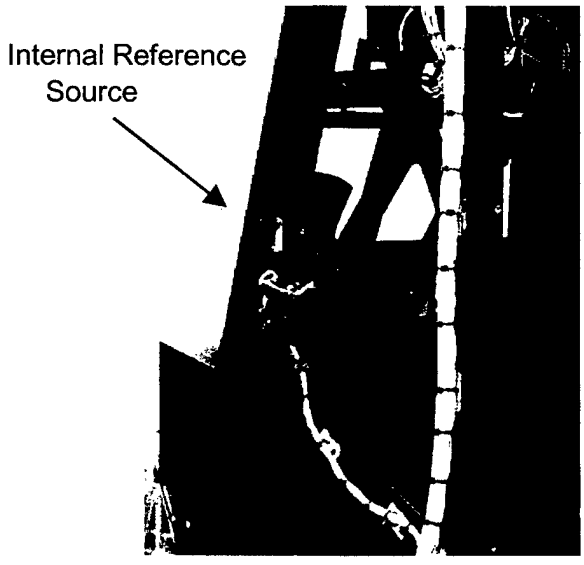

Figure 9. Photograph of internal reference source.

3. RADIOMETRIC STABILITY

The radiometric stability of the ALI has been tracked since launch using the techniques outlined above. Solar calibrations occur every two weeks and began on January 9, 2001. Lunar calibrations occur monthly and began on January 28, 2001. Ground truth measurements occur approximately every 2 months and began on December 30, 2000. Internal reference lamp measurements have been taken daily since November 25, 2000. However, only internal lamp measurements taken one day after focal plane bakeouts are used in stability analyses. Table 1 provides the dates for each of the calibrations and Figure 10 graphically represents their distribution.

Table 1. Dates of EO-1 ALI on-orbit radiometric calibrations.

Mission Day Number	Technique	Mission Day Number	Technique
5	Internal Lamp	192	Solar
11	Internal Lamp	197	Lunar
29	Internal Lamp	199	Internal Lamp
39	Ground Truth	207	Ground Truth
50	Internal Lamp	207	Internal Lamp
50	Solar	211	Solar
56	Internal Lamp	223	Ground Truth
61	Internal Lamp	227	Internal Lamp
63	Ground Truth	228	Lunar
67	Internal Lamp	234	Solar
73	Solar	237	Internal Lamp
73	Internal Lamp	239	Ground Truth
79	Lunar	248	Internal Lamp
79	Internal Lamp	249	Solar
81	Solar	257	Lunar
87	Solar	259	Internal Lamp
87	Internal Lamp	264	Solar
93	Internal Lamp	270	Internal Lamp
101	Internal Lamp	278	Solar
102	Solar	280	Internal Lamp
106	Internal Lamp	286	Lunar
110	Lunar	286	Ground Truth
114	Solar	291	Solar
114	Internal Lamp	291	Internal Lamp
120	Internal Lamp	301	Internal Lamp
128	Solar	306	Solar
128	Internal Lamp	313	Internal Lamp
134	Internal Lamp	317	Lunar
138	Lunar	320	Solar
142	Internal Lamp	322	Internal Lamp
143	Solar	328	Internal Lamp
149	Internal Lamp	332	Internal Lamp
156	Solar	334	Solar
158	Internal Lamp	343	Internal Lamp
168	Internal Lamp	345	Solar
169	Lunar	346	Lunar

Table 1. Dates of EO-1 ALI on-orbit radiometric calibrations. (Continued)

Mission Day Number	Technique	Mission Day Number	Technique
175	Ground Truth	353	Internal Lamp
179	Internal Lamp	360	Solar
180	Solar	366	Internal Lamp
188	Internal Lamp		

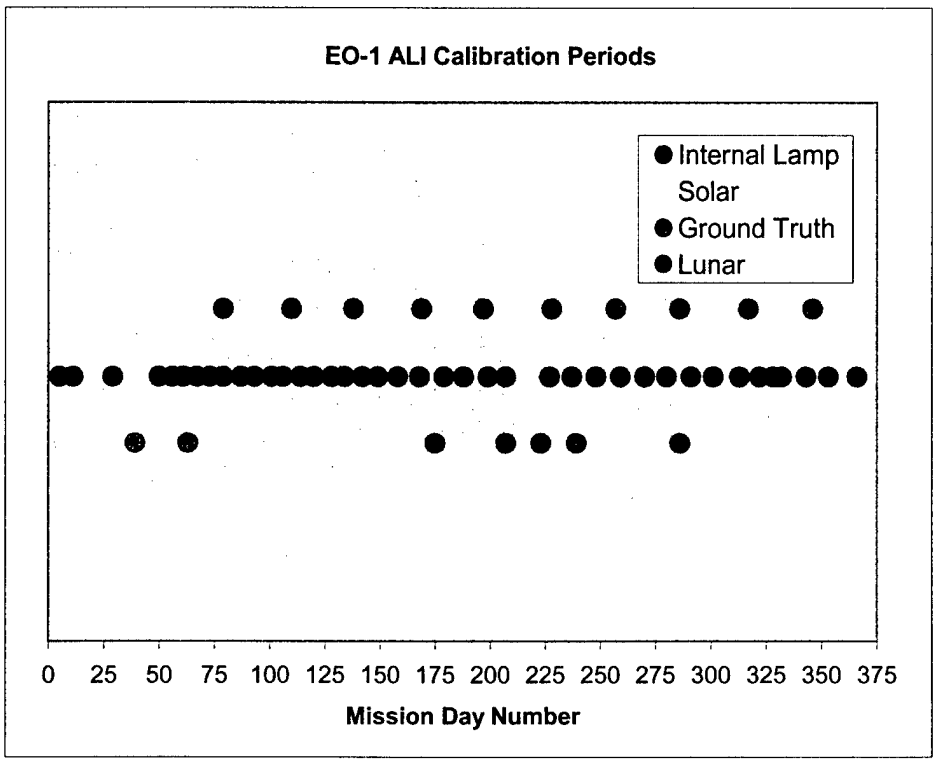

Figure 10. Radiometric calibration measurement periods.

All solar, lunar, and ground truth calibration data presented here have had corrections applied to remove the radiometric effects of contamination on the instrument focal plane filter surfaces. Contamination of the focal plane has been observed throughout preflight and on-orbit testing of the instrument. Fortunately, it has been demonstrated that by raising the temperature of the focal plane above 250 K, the effects of contamination are removed beyond measurable levels. However, between bakeout periods, a build-up of contaminants on the filter surfaces has been measured. These effects have been monitored daily on-orbit using the internal reference lamps. Figure 11 provides an example of the radiometric effects of contamination for Band 3 during the first year on-orbit.

Using the internal lamp data, a correction has been derived for each solar, lunar, and ground truth observation. This correction has been applied so that the intrinsic stability of the instrument may be tracked and compared using the various calibration techniques. Because the internal lamp data selected for trending is close to periods when the instrument is baked out, the effects of contamination are minimal for these data. The corrections applied to all bands are listed in Table 2.

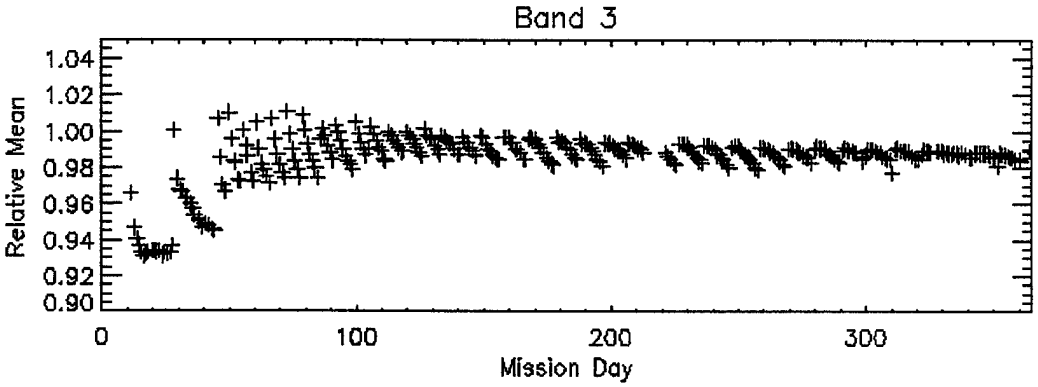

Figure 11. Effects of contamination on Band 3 data. Each point is derived from internal lamp data that has been ratioed to data obtained on Day 5 of the mission.

Table 2. Radiometric corrections (%) used to remove contamination effects.
(Ground truth panchromatic data were not available for this analysis.)

Method	Day Number	Band									
		1p	1	2	3	4	4p	5p	5	7	Pan
Lunar	79	0.19	0.19	0.12	0.26	0.06	0.08	-0.09	-0.01	0.00	0.01
	110	0.86	1.18	1.19	1.70	1.47	1.65	0.47	0.90	0.75	1.71
	138	0.40	0.66	0.74	0.98	0.70	0.90	0.19	0.57	0.34	1.28
	169	0.03	0.17	0.00	0.35	0.13	0.33	0.17	0.30	0.30	0.58
	196	0.31	1.46	1.14	1.65	1.60	1.82	0.76	1.11	0.88	1.60
	228	-0.03	-0.14	-0.12	0.23	-0.02	0.19	0.01	0.15	0.08	0.36
	257	0.91	1.41	1.19	1.52	1.33	1.55	0.54	0.87	0.72	1.58
	286	0.15	0.52	0.47	0.58	0.24	0.49	0.32	0.58	0.47	1.02
	317	-0.37	0.49	0.45	0.42	0.11	0.36	0.39	0.59	0.36	0.80
	346	-0.47	0.18	0.14	0.11	-0.25	-0.06	0.31	0.29	0.05	0.37
Solar	50	-0.83	0.11	0.24	0.90	0.91	0.85	0.17	0.18	-0.04	0.53
	73	0.02	0.19	0.24	0.55	0.37	0.37	-0.14	0.04	-0.03	0.40
	81	1.00	1.23	1.11	1.62	1.37	1.49	0.32	0.61	0.45	1.29
	87	-0.52	0.43	0.60	0.57	0.48	0.54	0.29	0.26	0.03	-0.42
	102	0.68	0.84	0.83	1.21	1.00	1.12	0.31	0.57	0.37	1.19
	114	-0.30	0.40	0.40	0.64	0.47	0.62	0.12	0.32	0.05	0.67
	128	0.34	0.26	0.23	0.41	0.18	0.36	-0.03	0.16	-0.02	0.69
	143	0.45	0.50	0.42	0.61	0.33	0.54	0.15	0.37	0.19	0.86
	156	0.21	1.27	0.98	1.48	1.37	1.62	0.71	1.17	1.04	1.68
	180	-0.55	0.21	-0.07	0.35	0.25	0.45	0.25	0.35	0.06	0.41
	192	0.48	0.39	0.42	0.81	0.59	0.81	0.45	0.66	0.43	1.13
	211	0.22	0.28	0.24	0.58	0.31	0.58	0.31	0.56	0.37	0.92
	234	0.49	0.88	0.84	1.08	0.84	1.11	0.45	0.82	0.69	1.46

Table 2. Radiometric corrections (%) used to remove contamination effects. (Continued)

Method	Day Number	Band									
		1p	1	2	3	4	4p	5p	5	7	Pan
	249	-0.66	0.12	0.03	0.28	0.08	0.32	0.25	0.34	0.20	0.40
	264	0.07	0.72	0.61	0.71	0.48	0.73	0.50	0.70	0.47	1.05
	278	-0.11	0.94	0.81	0.96	0.78	1.03	0.47	0.83	0.52	1.31
	291	-0.09	-0.20	-0.06	0.13	-0.20	-0.04	0.08	0.11	0.16	-0.27
	306	-0.25	0.59	0.48	0.47	0.15	0.41	0.32	0.57	0.36	0.85
	320	0.82	0.94	0.62	0.60	0.17	0.42	0.26	0.57	0.42	1.06
	334	-0.56	0.18	0.12	0.15	-0.17	0.00	0.28	0.30	0.19	0.42
	345	0.41	0.28	0.15	0.11	-0.33	-0.14	0.27	0.19	0.03	0.39
	360	-0.20	0.58	0.57	0.49	0.13	0.34	0.51	0.66	0.32	0.88
Ground Truth	38	1.88	3.31	3.43	5.53	4.48	4.55	2.74	4.92	6.05	NA
	63	0.44	1.62	1.60	2.58	2.47	2.58	0.76	1.13	0.87	NA
	175	0.85	1.20	0.98	1.46	1.25	1.49	0.55	1.02	0.81	NA
	205	-0.04	0.87	0.80	1.15	1.05	1.29	0.54	0.91	0.69	NA
	223	0.84	1.09	0.85	1.07	0.81	1.08	0.54	0.87	0.69	NA
	239	-0.08	0.07	0.06	0.36	0.06	0.33	0.18	0.35	0.22	NA
	286	0.15	0.52	0.47	0.58	0.24	0.49	0.32	0.58	0.47	NA
	307	0.70	0.74	0.61	0.55	0.13	0.40	0.30	0.60	0.52	NA

3.1 SOLAR CALIBRATION

Solar calibration data have been trended at the SCA and pixel level. Initially, all solar calibration data for aperture selector position six are ratioed to the data obtained on July 12, 2001. The mean of these ratios for each band and SCA is then plotted as a function of mission day number with standard deviations of the ratios used as 1-sigma error-bars. All data are normalized by the appropriate Sun-Earth distance correction factor corresponding to the day of the observation. The solar irradiance correction factor (F) is given by the approximation:

$$F = [1+e\cos((d-4)360°/365)]^2/[1-e^2]^2$$

where d is the day of the year and e = 0.01671 is the eccentricity of the Earth's orbit.

The distance correction factors used in this analysis are shown in Figure 12. Figure 13 depicts solar calibration results for SCA 1 of Band 3 for the first year on orbit. The original data as a function of mission day number is provided in the top graph. Normalized data are depicted in the second graph, and the residual errors to a linear fit to the data in the lower graph.

In order to identify sub-SCA response changes, a linear fit is performed on the data of individual detectors as a function of mission day number. The slope of each fit is then displayed as a function of cross-track position and examined for sub-SCA trends. Figure 14 depicts instrument level response changes as a function of cross-track position for Band 3 using the solar calibration technique.

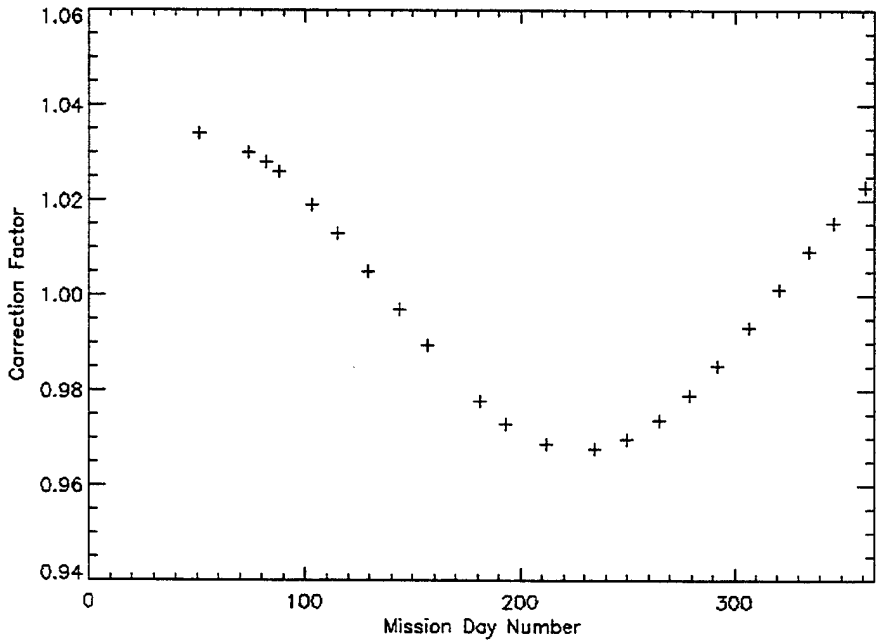

Figure 12. Solar calibration correction factors.

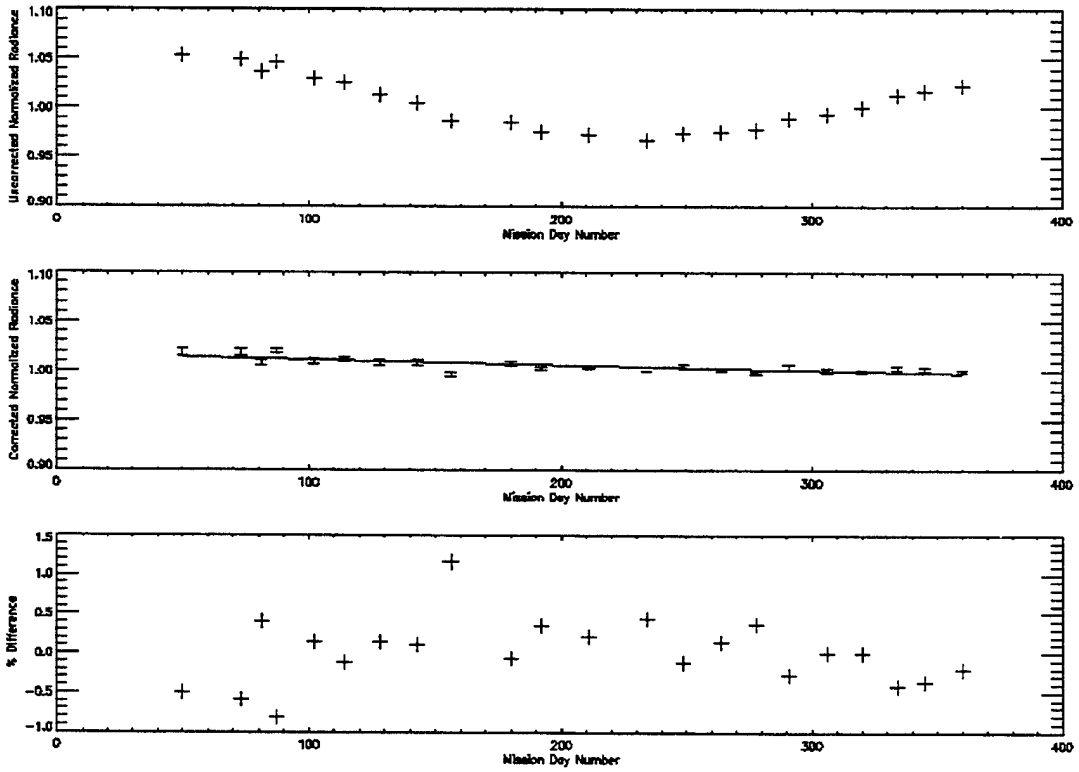

Figure 13. Instrument response stability for Band 3 based on solar calibration data.

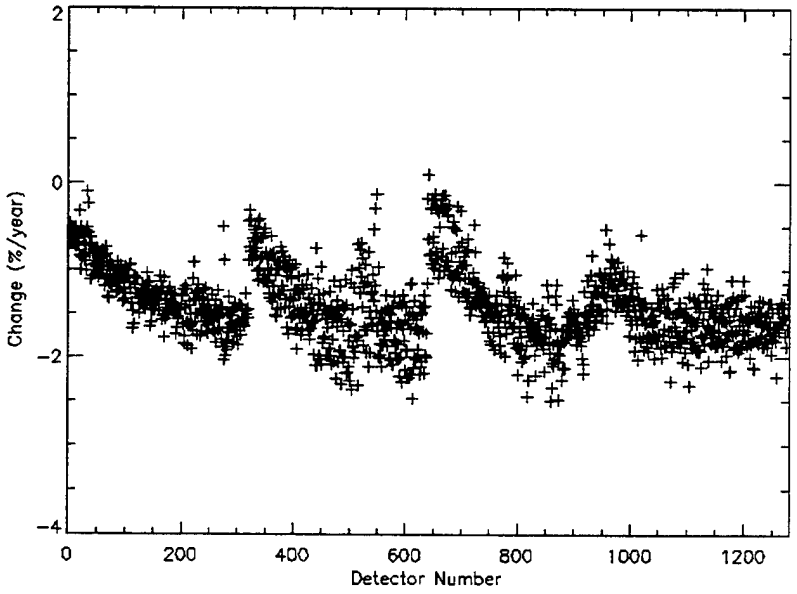

Figure 14. Change in instrument response for Band 3 derived from solar calibration data.

3.2 GROUND TRUTH

No correction factors are required to trend ground truth data. All Sun-Earth separation, atmospheric, and site reflectivity corrections are accounted for in the University of Arizona analysis. Unfortunately, because only a small region of a target may be characterized for an overflight, only portions of the focal plane may be sampled using the ground truth reflectance-based calibration techniques. Figure 15 depicts the ground truth data for Band 3 as a function of mission day number for the first year in the top graph and the residual errors to a linear fit to the data in the lower graph.

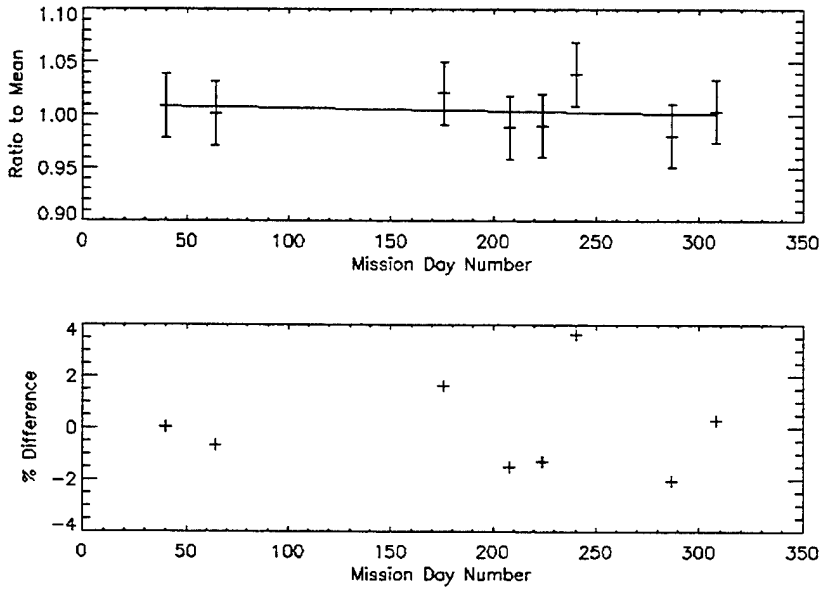

Figure 15. Instrument response stability for Band 3 based on ground truth measurements.

3.3 LUNAR CALIBRATION

No additional correction factors are required for lunar calibration trending. The spectral irradiance derived from ALI data is simply compared to the expected lunar irradiance, provided by the ROLO model. Because the Moon fills over 2/3 of an SCA, pixel level response changes cannot be monitored using this technique. However, SCA level trending may be accomplished and has been performed for the first year on orbit. Figure 16 depicts the lunar calibration data for Band 3 as a function of mission day number for the first year in the top graph and the residual errors to a linear fit to the data in the lower graph.

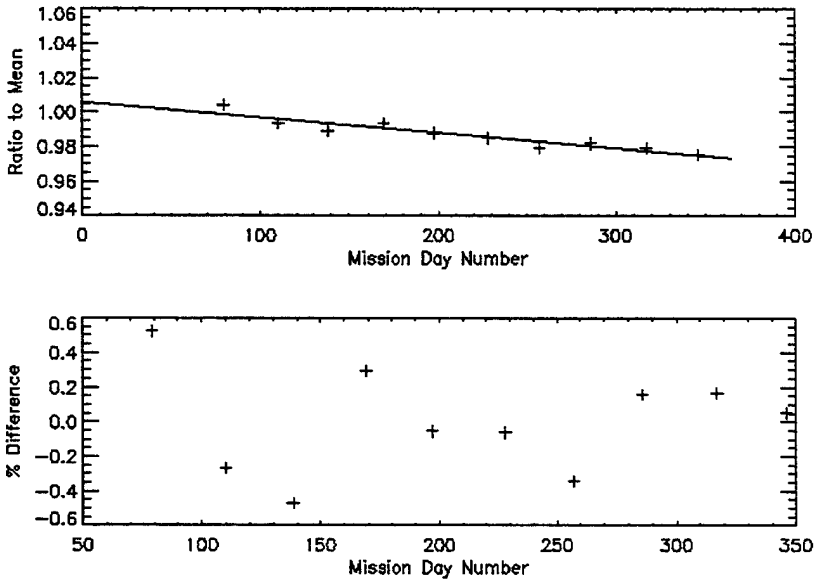

Figure 16. Instrument response stability for Band 3 based on lunar calibration measurements.

3.4 INTERNAL REFERENCE LAMP ILLUMINATION

Internal reference lamp data have been trended on the SCA and pixel level. Initially, all lamp data taken one day after each focal plane bakeout are ratioed to the data obtained on July 12, 2001. The mean of these ratios for each band and SCA is then plotted as a function of mission day number with standard deviations of the ratios used as 1-sigma error-bars. No correction factors are required to trend this data. Figure 17 depicts reference lamp results for Band 3 for the first year on orbit. The original data as a function of mission day number is provided in the top graph and the residual errors to a linear fit to the data in the lower graph.

In order to identify sub-SCA response changes, a linear fit is performed on the data of individual detectors as a function of mission day number. The slope of each fit is then displayed as a function of cross-track position and examined for sub-SCA trends. Figure 18 depicts instrument level response changes as a function of cross-track position for Band 3 using the reference lamp data.

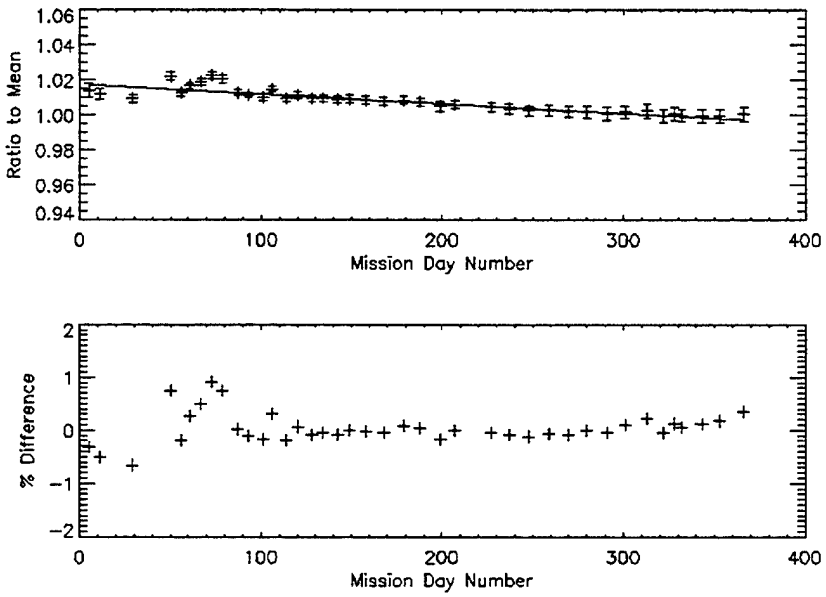

Figure 17. Band 3 instrument response stability based on internal reference lamp data.

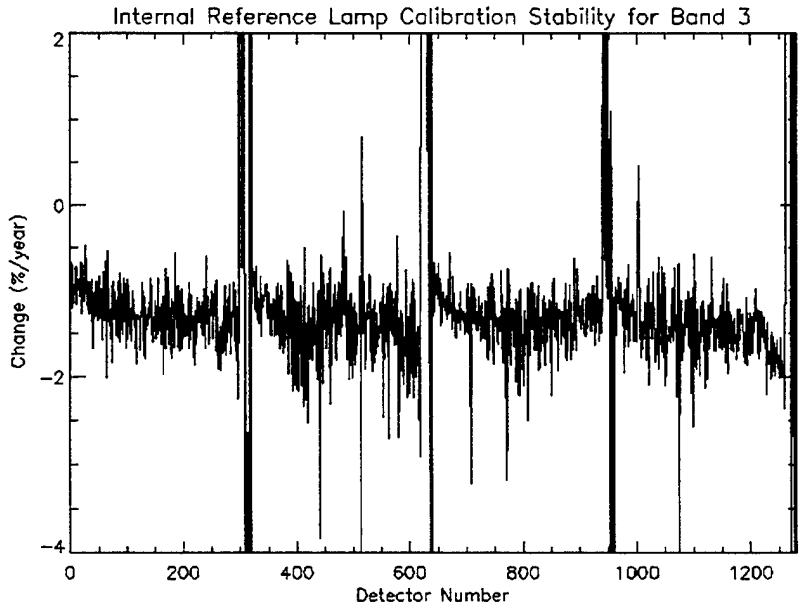

Figure 18. Change in instrument response for Band 3 derived from internal reference lamp data.

3.5 COMPARISON OF RESULTS

In an effort to compare results at the SCA level and derive additional information pertaining to the radiometric stability of the instrument from the combination of various calibration techniques, SCA 1 data for each band for all of the techniques described above have been overlaid in Figures 19–28. Linear fits to the data from combined internal lamp and solar calibration data are overlaid in each graph. Table 3 tabulates these results.

In order to compare sub-SCA trending, cross-track solar calibration and internal reference lamp data have been overlaid in Figures 29–38.

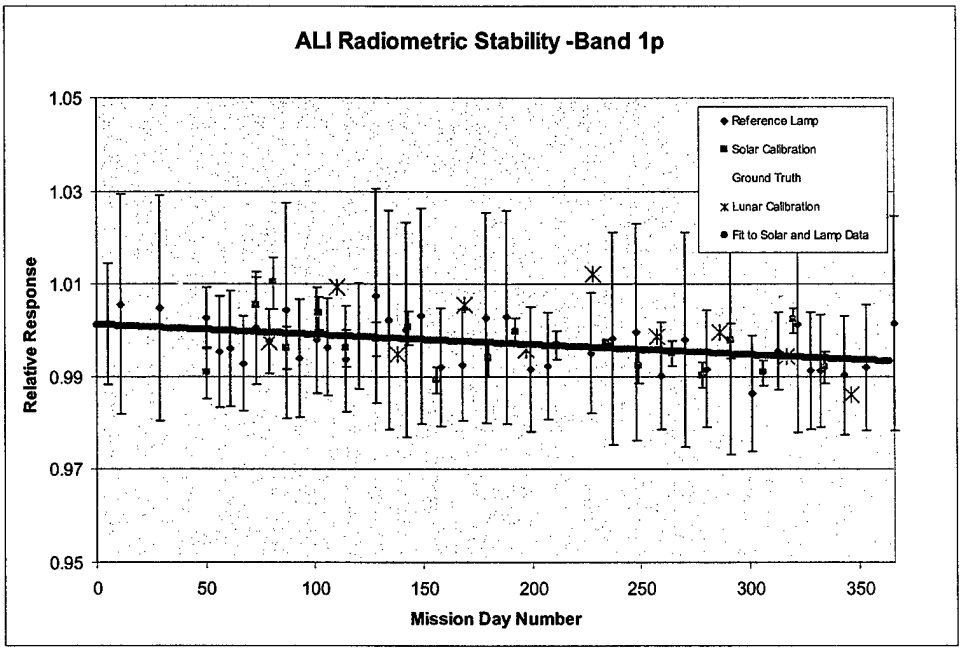

Figure 19. Trending of ALI radiometric calibration data for Band 1p.

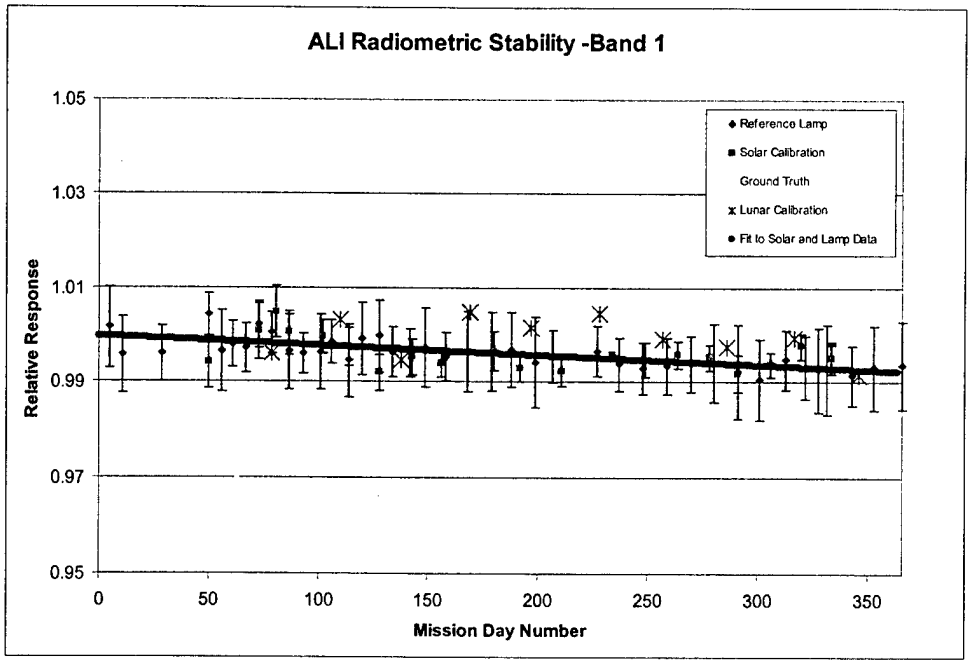

Figure 20. Trending of ALI radiometric calibration data for Band 1.

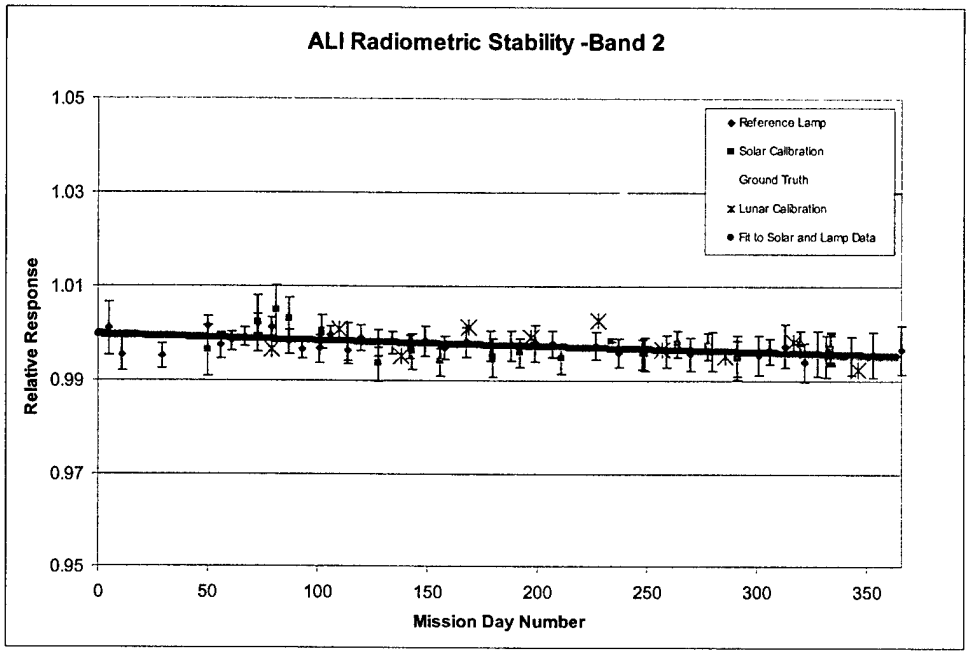

Figure 21. Trending of ALI radiometric calibration data for Band 2.

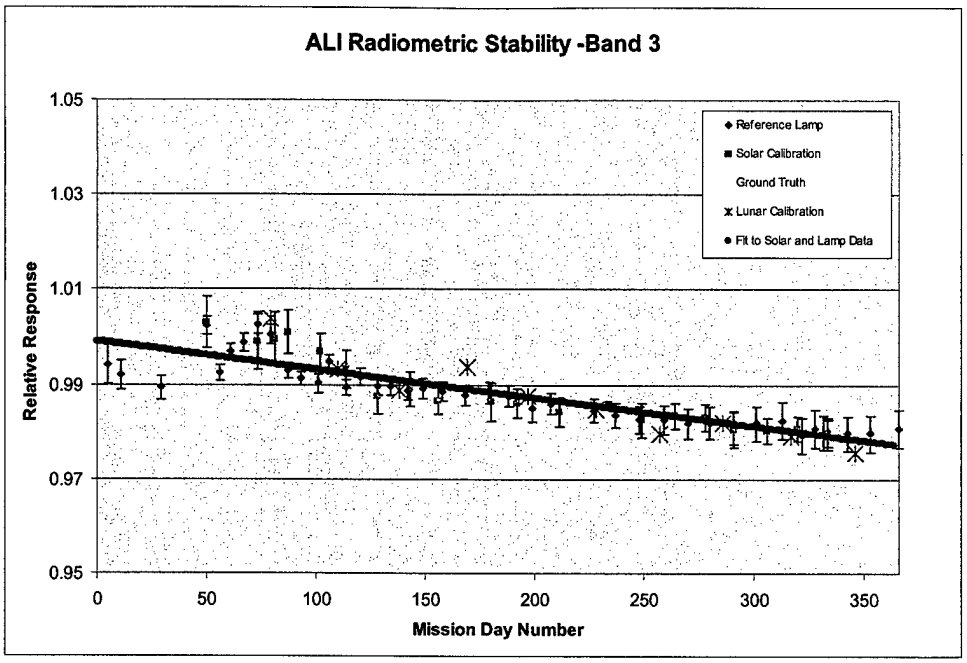

Figure 22. Trending of ALI radiometric calibration data for Band 3.

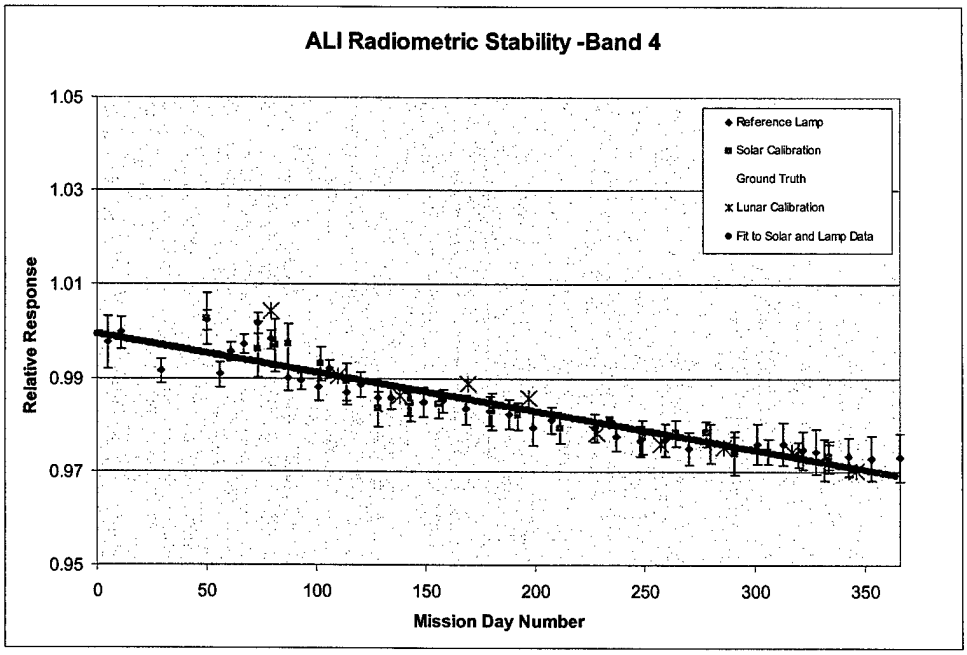

Figure 23. Trending of ALI radiometric calibration data for Band 4.

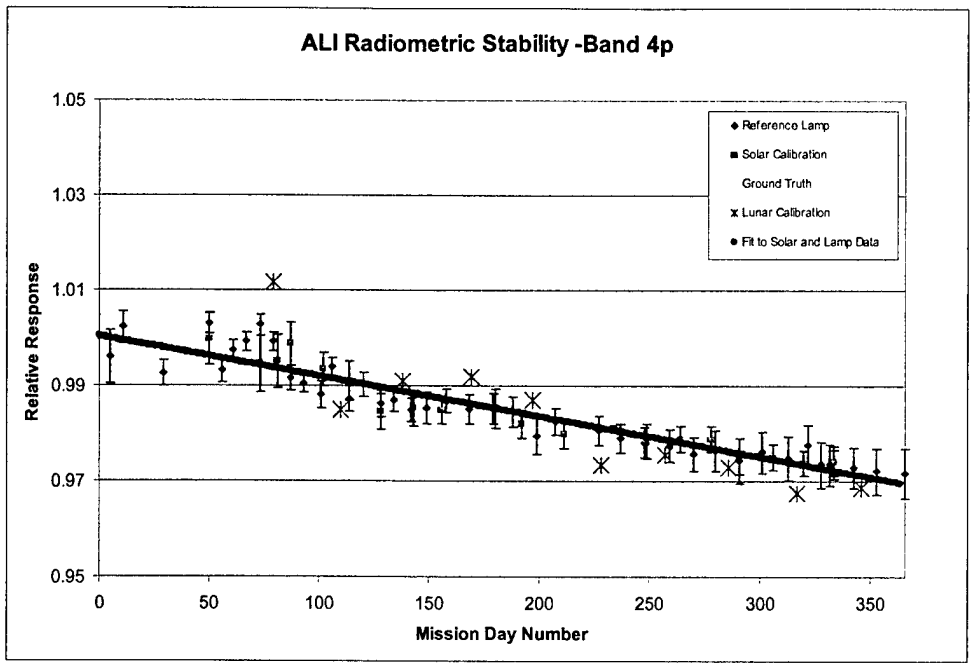

Figure 24. Trending of ALI radiometric calibration data for Band 4p.

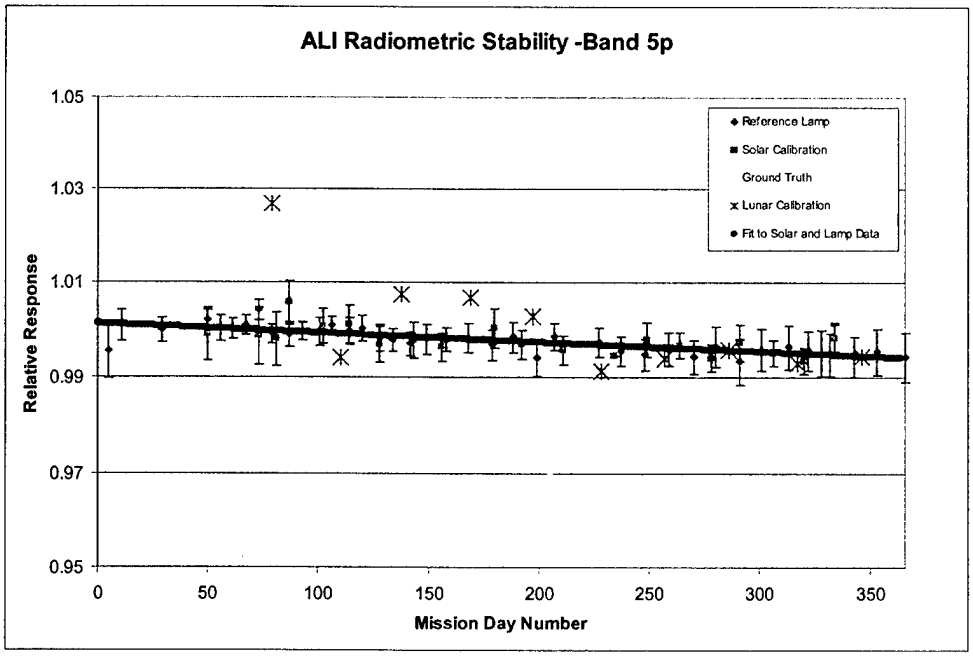

Figure 25. Trending of ALI radiometric calibration data for Band 5p.

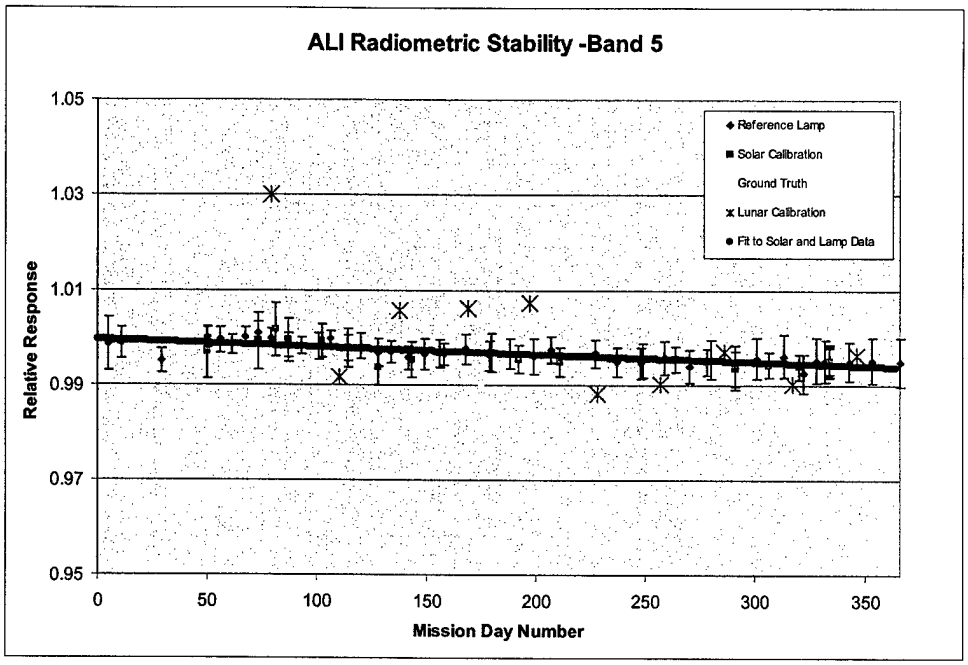

Figure 26. Trending of ALI radiometric calibration data for Band 5.

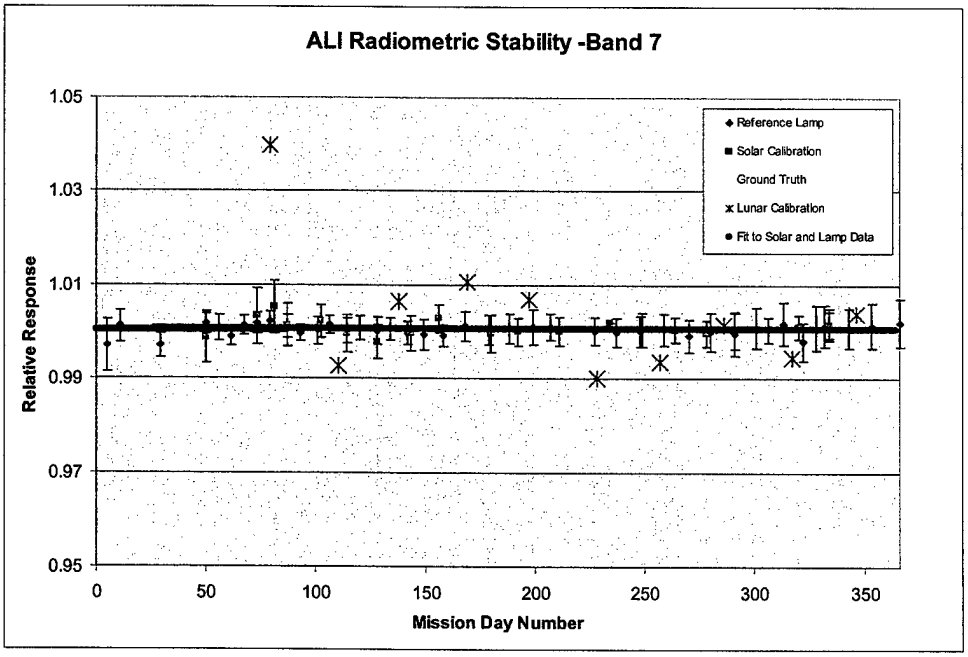

Figure 27. Trending of ALI radiometric calibration data for Band 7.

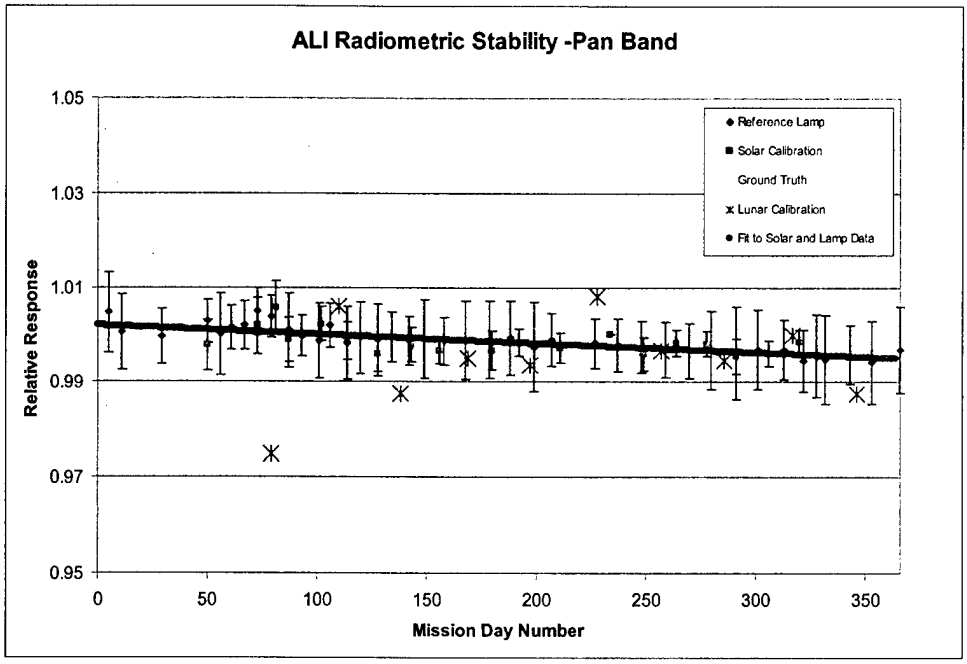

Figure 28. Trending of ALI radiometric calibration data for Pan Band.

Table 3. Radiometric stability trending results for first year on orbit.

Band	Response Change (%/year)
1p	-0.80
1	-0.75
2	-0.45
3	**-2.20**
4	**-3.04**
4p	**-3.10**
5p	-0.72
5	-0.59
7	0.02
Pan	-0.71

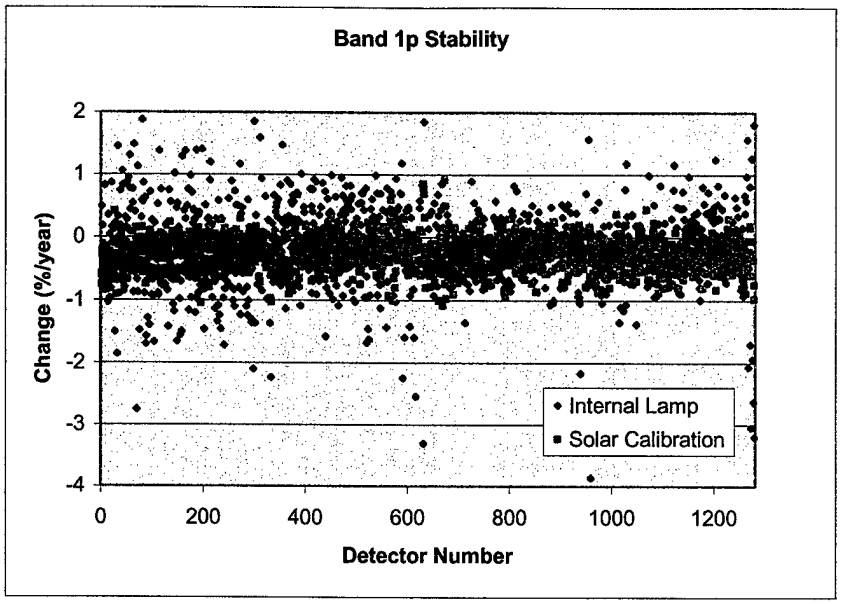

Figure 29. Radiometric stability of detectors for Band 1p as determined by internal lamp and solar calibration data collected during the first year on orbit.

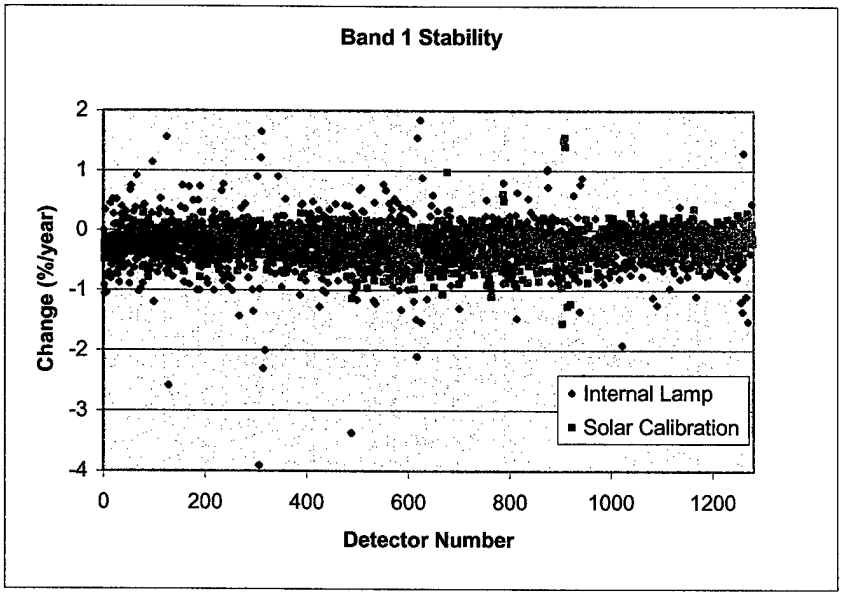

Figure 30. Radiometric stability of detectors for Band 1 as determined by internal lamp and solar calibration data collected during the first year on orbit.

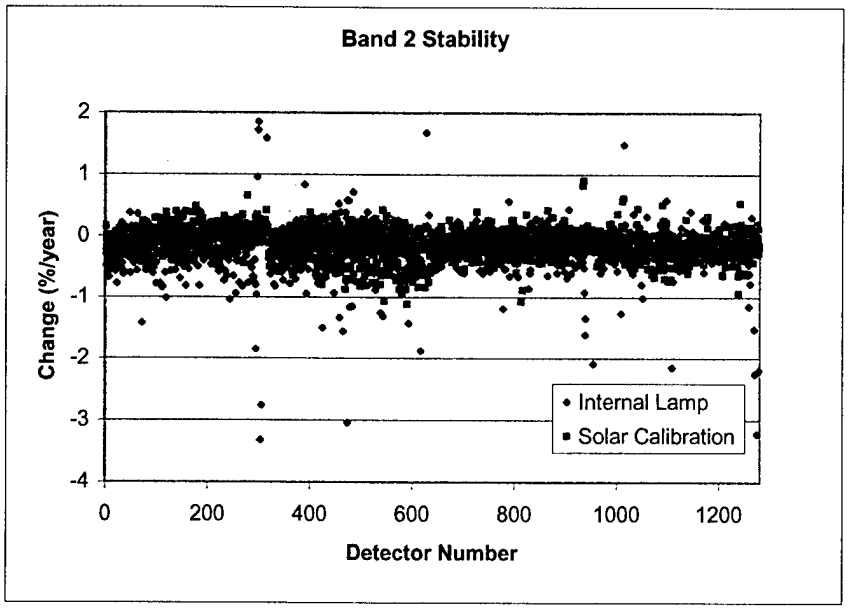

Figure 31. Radiometric stability of detectors for Band 2 as determined by internal lamp and solar calibration data collected during the first year on orbit.

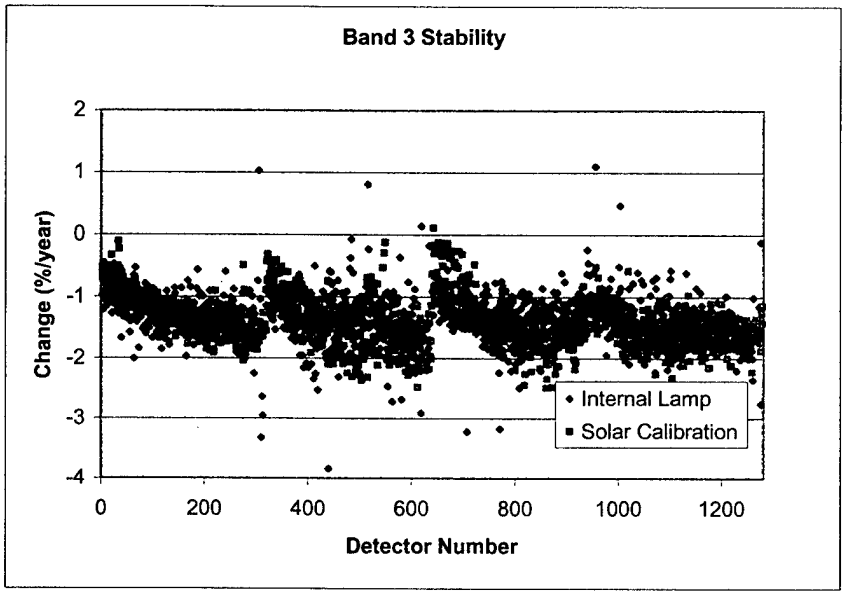

Figure 32. Radiometric stability of detectors for Band 3 as determined by internal lamp and solar calibration data collected during the first year on orbit.

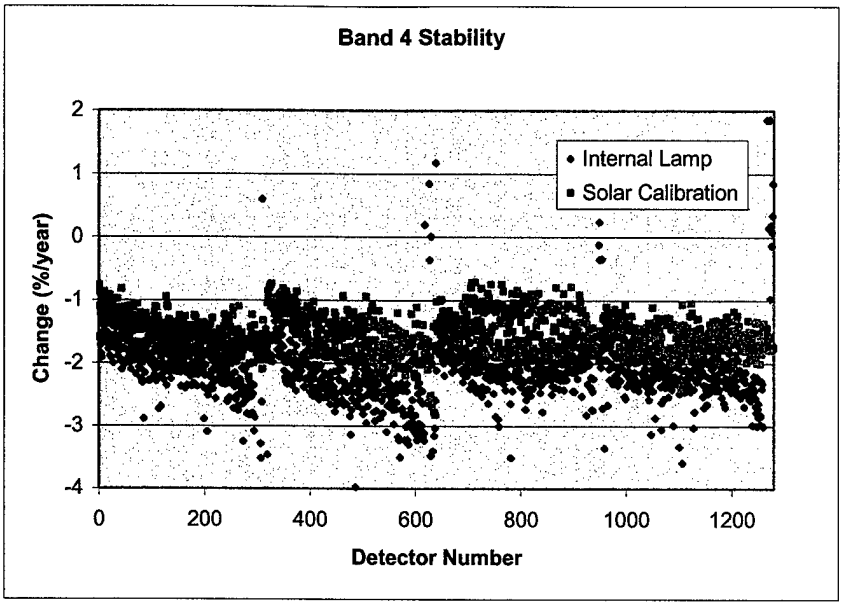

Figure 33. Radiometric stability of detectors for Band 4 as determined by internal lamp and solar calibration data collected during the first year on orbit.

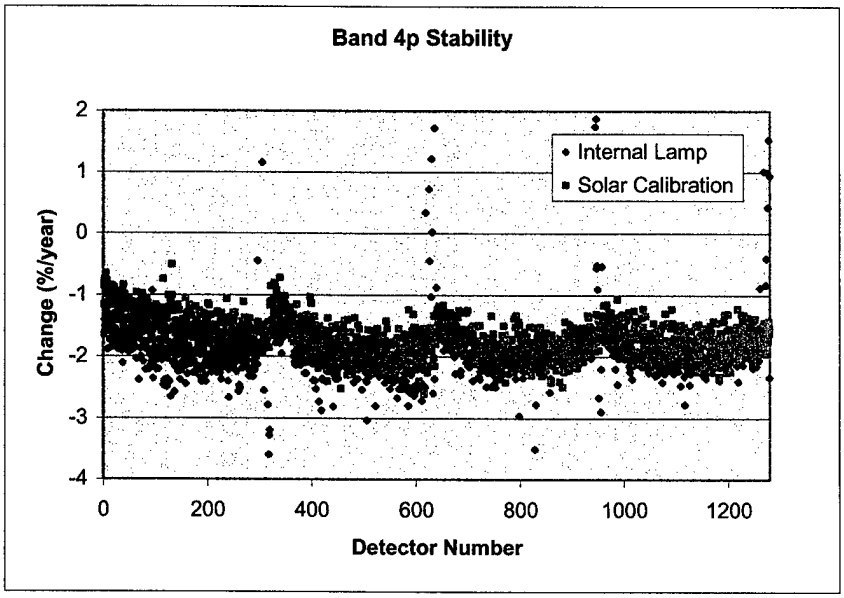

Figure 34. Radiometric stability of detectors for Band 4p as determined by internal lamp and solar calibration data collected during the first year on orbit.

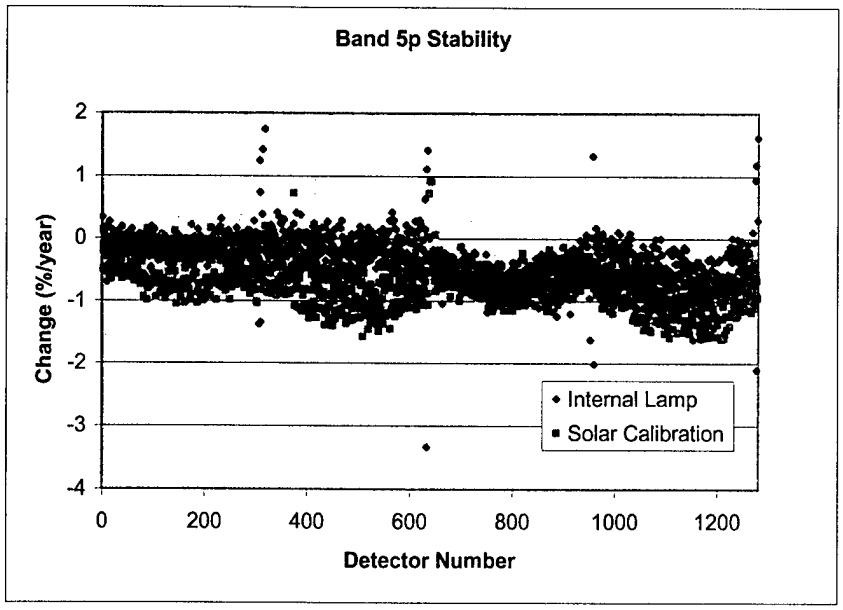

Figure 35. Radiometric stability of detectors for Band 5p as determined by internal lamp and solar calibration data collected during the first year on orbit.

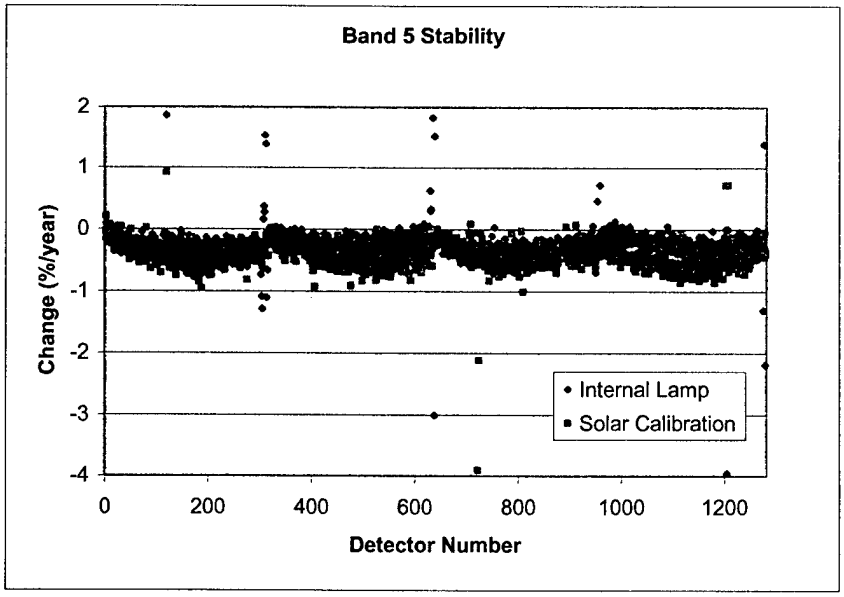

Figure 36. Radiometric stability of detectors for Band 5 as determined by internal lamp and solar calibration data collected during the first year on orbit.

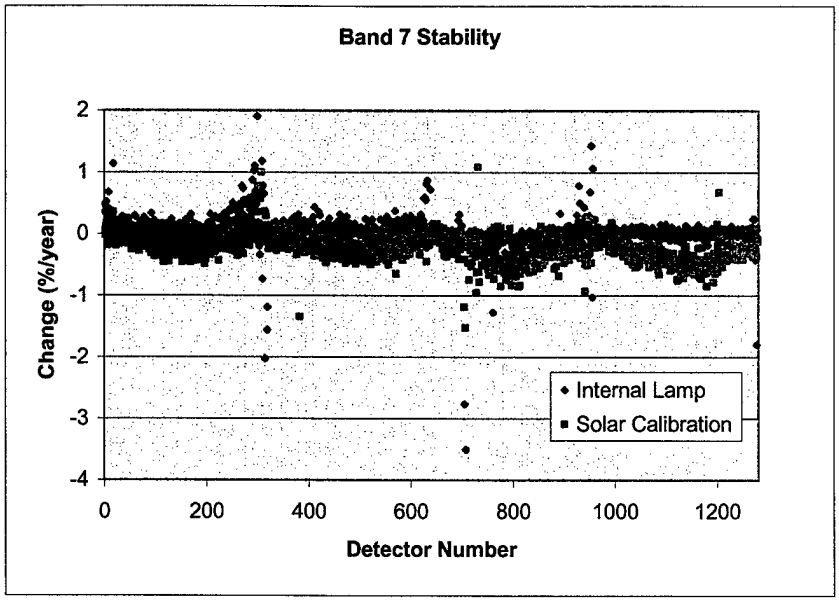

Figure 37. Radiometric stability of detectors for Band 7 as determined by internal lamp and solar calibration data collected during the first year on orbit.

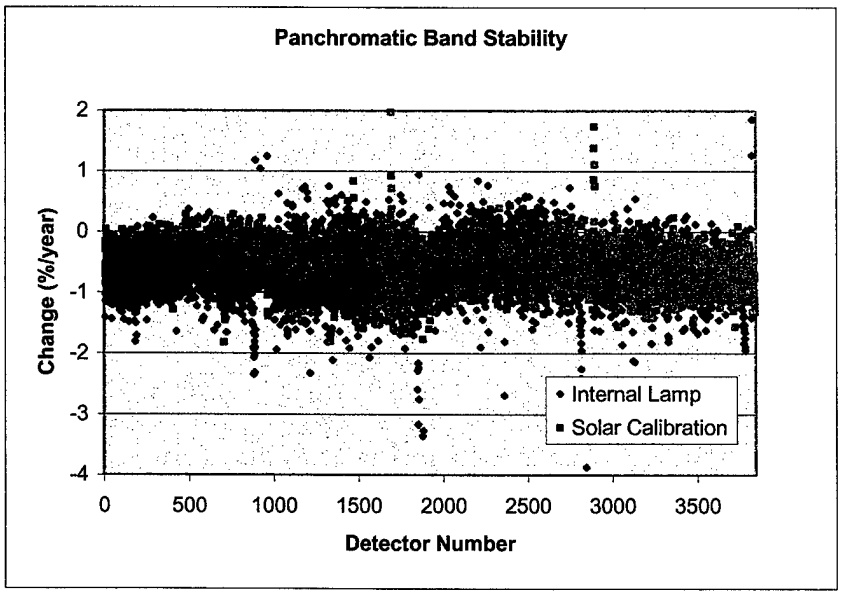

Figure 38. Radiometric stability of detectors for the panchromatic band as determined by internal lamp and solar calibration data collected during the first year on orbit.

4. DISCUSSION

The absolute radiometry of the Advanced Land Imager has been extensively examined during the first year the instrument was on-orbit using solar, lunar, and ground truth calibration techniques. Results from each method agree within experimental errors and indicate an 18% drop in the Band 1p response of the instrument since pre-flight characterization. Although one could argue the Spectralon diffuser used in the solar calibration technique could have become contaminated during ground testing or launch, radiometric calibration data that do not involve the diffuser (e.g. ground truth and lunar observations) also observe a similar Band 1p change. This exonerates the diffuser and suggests the change has occurred elsewhere in the instrument. Additionally, because the solar calibration technique does not employ the secondary mirror, this component is the only element within the optical chain that cannot be responsible for the observed change.

The on-orbit calibration data also reveal a small drooping of the other VNIR band responses (other than Band 1p) towards the blue. The highest of these is a 5% decrease in radiometric response for Band 1. Again, because ground truth, lunar and solar data reveal similar changes, only the diffuser and secondary mirror can be eliminated as sources for these changes.

Finally, the on-orbit Band 5 response is consistently 5–12% higher than the response measured during pre-flight calibration. It is interesting to note the change in response as determined from the solar and lunar calibration techniques are consistently 7% lower than those calculated from ground truth data. The source of this difference is not understood at this time.

4.1 SOURCES OF RADIOMETRIC DIFFERENCES

There are several possible sources of the radiometric discrepancies between preflight and flight measurements. The three leading candidates are 1) errors in the preflight calibration of the instrument, 2) stray light, and 3) a change in the instrument response. The preflight radiometric calibration of the ALI is based on the knowledge of the radiance emitted by a 30-inch-diameter integrating sphere at several emission levels. To validate this knowledge, the NASA/Goddard developed Landsat Transfer Radiometer (LXR)[8] was brought to Lincoln Laboratory and used to measured the sphere radiance. The LXR measurements agreed with the pre-flight spectroradiometer measurements to within ±2% for all eight of the LXR VNIR bands for three sphere intensity levels. This agreement includes an LXR band 10 nm wide centered at 440 nm, equivalent to Band 1p of the ALI. The good agreement suggests the pre-flight calibration of the ALI was well understood and measurement uncertainties cannot account for the apparent radiometric changes on orbit in the VNIR.

Another possible source of error in ALI radiometry on orbit is stray light. One technology being demonstrated by the ALI is large, wide field-of-view, silicon carbide optics. Another possible source of error in ALI radiometry on orbit is stray light. The ALI has poor stray light performance as a result of the mirror finish on the primary and tertiary mirrors, scatter from the black paint lining the interior of the telescope, and focal plane filter scatter. A system level model of these effects has been developed to assess the impact of stray light on flight observations. This model has been verified using flight data. The effects of stray light can be significant for dim regions of scenes with high contrast. However, it can be stated that the effects of stray light on the absolute radiometric data presented here are small. Solar and internal lamp data are diffuse scenes obtained with the aperture cover closed. Ground truth and lunar observations are bright targets in dim backgrounds, minimizing the effects of stray light from outside the target field.

Extensive preflight measurements of the BRDF for the optical elements were made and these data were used in a system level analysis to assess the impact of stray light on flight observations. A model was developed to estimate the error in measured scene radiance as a function of the ratio of target radiance to background radiance. This effect can be significant for dim regions of scenes with high contrast. The details of the characterization and effects of stray light on flight data are presented elsewhere[9]. However, it can be stated that the effects of stray light on absolute radiometric data presented here are small. Solar and internal lamp data are diffuse scenes obtained with the aperture cover closed. Ground truth and lunar observations are bright targets in dim backgrounds, minimizing the effects of stray light from outside the target field.

The final source of observed discrepancies between preflight and flight calibration measurements is a real response change within the instrument. This includes a change in the reflectivity of the mirrors, the spectral bandpasses of the filter assemblies, or the responsivity of the detector arrays. Contamination of the top surface of the focal plane filters has been detected since initial instrument thermal vacuum testing. Trending of internal lamp data indicate that a gradual build-up of material occurs when the focal plane is operated below 250 K. This data also reveals that the contaminant is virtually removed by raising the temperature of the focal plane for a 20-hour period every ten days on orbit. This chronic problem raises suspicions relating to the apparent permanent change in instrument response since preflight calibration. However, internal reference lamp trending indicates the reflectivity of flat mirror (M4) and the response of the focal plane have remained stable to within 1% for bands 1p, 1, 2, 5p, 5, 7, pan, and within 3% for bands 3, 4, 4p since launch. Unfortunately, the observed increase in internal lamp intensity after launch prohibits one from extending focal plane response trending from preflight calibration to on orbit. However, trending does exist from preflight calibration at Lincoln Laboratory in December 1998 through the second spacecraft thermal vacuum test at Goddard Space Flight Center in July 2000 (4 months before launch). This data indicates M4 and the focal plane have remained stable to within 2% during ground testing. Furthermore, solar, lunar, and ground truth data trending, which exercise other elements of the optical train, suggest M1, M2, M3, and the solar diffuser have been stable to within 1% since the first on-orbit calibrations in late December 2000. As a result, if a response change did occur within the instrument, it must be restricted to between July 2000 and November 21, 2000 if the change occurred on M4 or the focal plane or it must be restricted to between December 1998 and December 29, 2000 if the change occurred on M1, M2, or M3.

Although the cause of the preflight to flight radiometric calibration discrepancy is not clearly understood, the stability of the instrument suggests a single radiometric correction to the preflight calibration coefficients for each band will provide ±5% agreement between measured solar, lunar and ground truth data and expected values during the first year on orbit. Each band's correction factor has been derived by first developing a calibration error model as a function of the ratio of target to background radiances for a variety of scenes by comparing Landsat 7 ETM + data to ALI data and including solar, lunar, and ground truth measurements. The target radiance is defined as the mean radiance of a small region of interest, usually only tens of pixels in diameter. The background radiance is defined as the mean radiance of a three-degree region centered on the target. This error model includes effects of stray light and absolute radiometric offsets. A detailed description of the calibration error model is described elsewhere[9]. Figure 39 depicts the calibration error model developed for Band 3, overlaid with flight data. Once the model is defined, a band's absolute radiometric correction factor is defined as the calibration error for a target to background ratio of 1.0. In order to account for the observed slight linear decrease in radiometric response revealed in the stability data, the correction factors are then normalized to the predicted June 1, 2001 response level for each band.

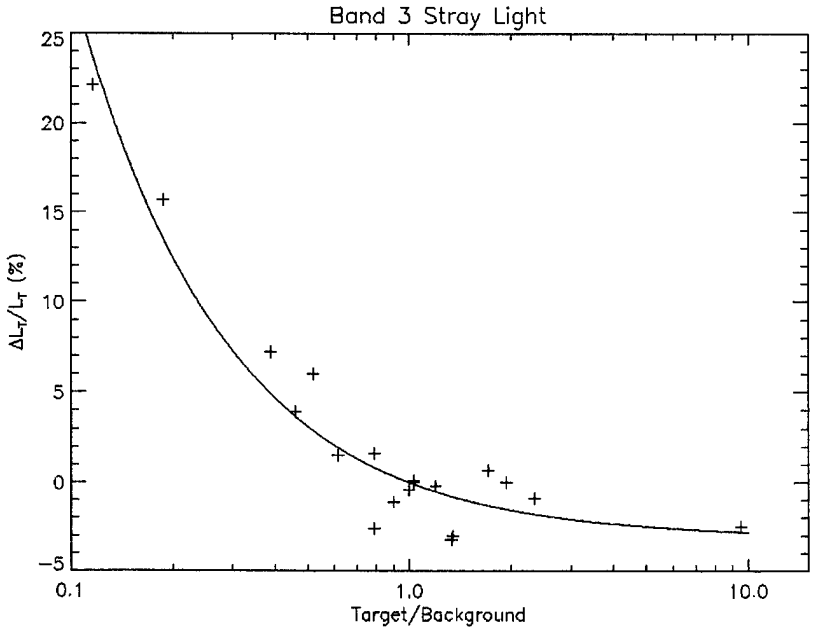

Figure 39. Band 3 radiometric error model and flight data.

Table 4 lists the radiometric correction factors derived using the above technique. These factors have been used to update the preflight radiometric coefficients residing in the EO-1 ALI Radiometric Calibration Pipeline. Figure 40 depicts the results of solar, lunar, and ground truth testing once the on-orbit data has been processed using the updated calibration coefficients. As one may see, the agreement between the methods of calibration outlined above to ALI observations using the new coefficients is within ±5% for all bands, except Band 5. For this band the solar and lunar calibration data still differ from ground truth data by 7%.

Table 4. Radiometric correction factors used to update preflight calibration coefficients.

Band	Correction Factor
1p	1.21
1	1.07
2	1.05
3	1.04
4	1.02
4p	0.99
5p	0.98
5	0.87
7	0.98
Pan	1.05

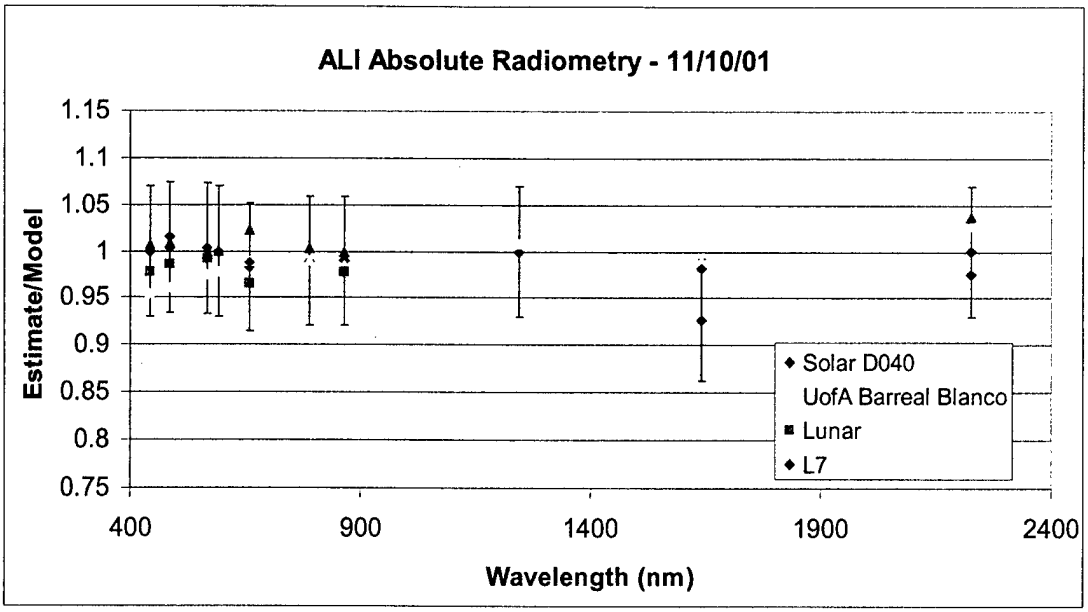

Figure 40. Results of ALI absolute radiometric calibration after the corrections to pre-flight calibration coefficients are applied.

4.2 STABILITY

The ALI stability measurements using solar, lunar, ground truth, and internal lamp data are in good agreement. All methods indicate excellent stability (<1 %/year) for Bands 1p, 1, 2, 5p, 5, 7, pan. However, solar and lunar data indicate a 2-3% change per year for Bands 3, 4, 4p. Because the internal lamp data also track this trend, these changes can be isolated to the flat mirror and/or focal plane. Ground truth data also suggest these trends, but longer timelines are necessary to strengthen this result.

The Band 3, 4, 4p linear decrease in response should be monitored and correction factors applied to these data as a function of mission day number in order to preserve the absolute radiometric accuracy of ALI data for these bands.

Stability measurements also reveal 1%/year long-term intra-SCA variations for Bands 3, 4, 4p (Bands 5p, 5, 7 to a lesser degree). These variations are consistent between solar and internal lamp data, isolating the source to the flat mirror and/or the focal plane. These variations appear similar to the effects of contamination build-up observed during preflight calibration of the instrument. This suggests a slow, low-level build-up of a contamination layer may be occurring on the focal plane filter surfaces for these bands. This effect will result in the degradation of the ALI detector-to-detector radiometric accuracy or 'flat-fielding' as a function of mission day number. This will manifest itself as 1) 'cusping' within an SCA and 2) SCA to SCA boundaries becoming evident for scenes that would normally be considered radiometrically flat. These effects can be mitigated by correcting the intra-SCA radiometric calibration coefficients every six months.

4.3 CALIBRATION METHODS

Of the four radiometric calibration techniques described above, the internal reference lamps and the solar calibration methods are the simplest. Although the internal reference lamps are very stable, the apparent increase in lamp brightness after launch resulted in the loss of the absolute radiometric transfer capability from preflight to on-orbit. Additionally, these lamps only sample the flat mirror and the focal plane and cannot be used as a monitor of the overall instrument stability. However, they have proven to be extremely valuable in tracking the build-up of contamination on the focal plane filters and also in monitoring the focal plane stability on a daily basis. Additionally, because the reference lamps illuminate most of the focal plane, analysis of these data may be used to identify sub-SCA radiometric response changes.

The solar calibration technique is particularly attractive since it requires only the Sun-Earth $1/r^2$ distance correction factor to trend data as a function of time. Additionally, this method provides a seven point radiometric linearity check for each detector for most bands and provides a means for identifying sub-SCA response changes at the instrument level. Although this technique does employ a Spectralon diffuser that is easily contaminated, the location of the diffuser within the telescope cavity helps to shield the diffuser surface from spacecraft contaminants as well as Solar and Earth-reflected ultraviolet radiation.

Lunar calibration is an attractive radiometric calibration method since the Moon is geologically stable and spectrally flat. The data presented here also suggest lunar observations are a good tool for tracking the stability of the instrument. However, this technique is only now maturing and being integrated into spacecraft calibration plans. As a result, uncertainties related to the absolute calibration of the moon still exist at this time. Furthermore, the lunar calibration method can only be used to identify radiometric response changes for detectors illuminated by the lunar disk and for the region of the focal plane used to integrate the lunar signal.

Perhaps the most complex method of absolute radiometric calibration is the ground-based reflectance method. This requires precise field measurements, atmospheric modeling, and radiative transfer propagation in order to account for temporally varying surface reflectivities and atmospheric conditions. Furthermore, this method is restricted to the region of the scene characterized by the field measurements and cannot be used to identify response changes for the entire ALI field of view. However, once the absolute radiometric calibration of a portion of an instrument's response has been accomplished, the remaining response may also be calibrated by observing large flat scenes and bootstrapping the ground truth results to the observation. Additionally, the reflectance method is critical for validating solar and lunar calibration data and in some cases is the only method available for monitoring the radiometric accuracy and stability of instruments whose on-board calibration systems had failed or become unreliable.

REFERENCES

1. D. E. Lencioni, C. J. Digenis, W. E. Bicknell, D. R. Hearn, and J. A. Mendenhall, "Design and Performance of the EO-1 Advanced Land Imager," *SPIE Conference on Sensors, Systems, and Next Generation Satellites III*, Florence, Italy, 20 September 1999.
2. J. A. Mendenhall et al., "Earth Observing-1 Advanced Land Imager: Instrument and Flight Operations Overview," MIT/LL Project Report EO-1-1, 23 June 2000.
3. D. E. Lencioni, J. A. Mendenhall, D. P. Ryan-Howard, "Solar Calibration of the EO-1 Advanced Land Imager," IGARSS 2001, Sydney, 9 July 2001.
4. J. A. Mendenhall, D. E. Lencioni, J. B. Evans, "Earth Observing-1 Advanced Land Imager: Radiometric Response Calibration," MIT/LL Project Report EO-1-3, 29 November 2000.
5. Thome, K.J., "Absolute radiometric calibration of Landsat 7 ETM+ using the reflectance-based method," Remote Sensing of Environment, 78, 2001, 27-38.
6. Bigger, S. F., Private Communication, May 2001.
7. Keiffer, H.H, Anderson, J.A., "Use of the Moon for spacecraft calibration over 350-2500 nm," Proc. SPIE, 2438, 325-335, 1998.
8. Brian Markham, Private Communication, September 2000.
9. J. A. Mendenhall and D. E. Lencioni, "EO-1 Advanced Land Imager Stray Light Analysis and Impact on Flight Data," IGARSS 2002, Toronto, June 24, 2002.

REPORT DOCUMENTATION PAGE

Form Approved
OMB No. 0704-0188

1. AGENCY USE ONLY (*Leave blank*)	2. REPORT DATE	3. REPORT TYPE AND DATES COVERED
	31 May 2001	Project Report

4. TITLE AND SUBTITLE

Earth Observing-1 Advanced Land Imager Flight Performance Assessment: Absolute Radiometry and Stability During the First Year

5. FUNDING NUMBERS

C—F19628-00-C-0002

6. AUTHOR(S)

J.A. Mendenhall, D.E. Lencioni

7. PERFORMING ORGANIZATION NAME(S) AND ADDRESS(ES)

Lincoln Laboratory, MIT
244 Wood Street
Lexington, MA 02420-9108

8. PERFORMING ORGANIZATION REPORT NUMBER

PR-EO-1-10

9. SPONSORING/MONITORING AGENCY NAME(S) AND ADDRESS(ES)

NASA/GSFC
Mr. Ralph Welsh
Building 16, Room 21 MS740.3
Greenbelt, MD 20771

10. SPONSORING/MONITORING AGENCY REPORT NUMBER

ESC-TR-2001-071

11. SUPPLEMENTARY NOTES

None

12a. DISTRIBUTION/AVAILABILITY STATEMENT

Approved for public release; distribution is unlimited.

12b. DISTRIBUTION CODE

13. ABSTRACT (*Maximum 200 words*)

The absolute radiometry of the Advanced Land Imager during the first year on orbit (November 21, 2000 - November 21, 2001) is presented. Results derived from solar, lunar, ground truth, and internal reference lamp measurements are presented. An 18% drop in the radiometric response of the Band 1p data since preflight calibration at Lincoln Laboratory is observed using all techniques. This decrease cannot be accounted for by preflight calibration errors, stray light, or contamination of the focal plane. A slight drooping of the VNIR response toward the blue and a 5-12% increase in the Band 5 response is also apparent in all the data. Radiometric response correction factors have been calculated and preflight calibration coefficients have been updated in order to provide ±5% agreement between the measured solar, lunar, and ground truth data and the expected values.

The radiometric stability of the ALI during the first year of operation is also presented for each spectral band. Internal reference lamp data indicate the focal plane has been stable to within 1% for bands 1p, 1, 2, 5p, 5, 7, pan and 3% for Bands 3, 4, 4p since launch. Solar, lunar, and ground truth measurements indicate the optical train and solar diffuser of the instrument has been stable to within 1% since initial measurements on orbit in late December 2000.

14. SUBJECT TERMS

15. NUMBER OF PAGES
40

16. PRICE CODE

17. SECURITY CLASSIFICATION OF REPORT	18. SECURITY CLASSIFICATION OF THIS PAGE	19. SECURITY CLASSIFICATION OF ABSTRACT	20. LIMITATION OF ABSTRACT
Unclassified	Unclassified	Unclassified	Same as Report